Joaquín José Vieiro Medina

Flexible Pipes: Slug Flow and Structure Coupling

Joaquín José Vieiro Medina

Doctoral Thesis

NTNU
Norwegian University of
Science and Technology
Faculty of Engineering
Department of Energy and Process Engineering

◉ NTNU
Norwegian University of
Science and Technology

◉ NTNU

◉ NTNU
Norwegian University of
Science and Technology

Joaquín José Vieiro Medina

Flexible Pipes: Slug Flow and Structure Coupling

Thesis for the degree of Philosophiae Doctor

Trondheim, October 2018

Norwegian University of Science and Technology
Faculty of Engineering
Department of Energy and Process Engineering

◼ NTNU
Norwegian University of
Science and Technology

Preface

This thesis is submitted for partial fulfilment of the requirements for the degree of Philosophiae Doctor (Ph.D.) at the Norwegian University of Science and Technology (NTNU).

The work has been performed at the Department of Energy and Process Engineering in the Faculty of Engineering. Professor Ole Jørgen Nydal has been the main supervisor, while Professors Svein Sævik and Carl Martin Larsen from the Department of Marine Technology were co-supervisors.

Abstract

In this thesis, a computational scheme for coupled internal multiphase flow and structural dynamic of flexible pipes is presented and tested. The model consists of a 1D simulator based on a slug tracking model, and a 3D structural dynamic simulator based on lumped mass formulation. Internal fluids weight, friction and centrifugal force were integrated in the structural analysis as well as environmental forces such pipe-soil contact and external drag, among others.

The models were coupled using a domain-decomposition method where the structure and the flow are computed independently using separated solvers and data is transmitted between them in order to include coupling effects. The resulting software is a stand-alone application capable of predicting the two-way coupling of multiphase flow in flexible pipes.

The coupled model has been tested by comparing simulations with experimental data from small scale setups. Different scenarios were studied such as floating pipe, submerged lazy wave shaped pipe, pigging of a submerged pipe, garden hose instability and a blowout case. The developed model was able to reproduce qualitatively or quantitatively key features observed during the experimental tests.

Acknowledgements

Contents

List of Figures

List of Tables

Chapter 1

Introduction

1.1 Motivation

Flexible pipes are often used in offshore oil and gas production systems to transport the well fluids from the seabed to surface facilities. These flexible pipes are exposed to multiple external loads like sea current drag, vortex shedding induced forces, waves and seabed interaction together with forces due to the internal flow such as gravitational loads and flow momentum variation, among others.

As well fluids are often comprised of a mixture of different fluid and solid phases (gas, oil, water and sand), diverse flow patterns may arise. A flow pattern is characterized by geometrical configurations of the phases in a section of pipe, and depends on operational (flow rates) and geometrical variables (pipe diameter and inclination), as well as physical properties of the phases [1]. In horizontal pipes, the flow patterns has been classified as stratified flow, intermittent flow, annular flow and disperse bubble flow. In vertical pipes the stratified regime disappears and the churn flow appears. Figure 1.1 and Figure 1.2 show the most common flow pattern definitions for horizontal and upward vertical gas-liquid flow in pipes.

Stratified

Stratified-Smooth

Stratified-Wavy

Intermittent

Elongated-Bubble

Slug

Annular

Annular

Wavy-Annular

Dispersed-bubble

Dispersed- bubble
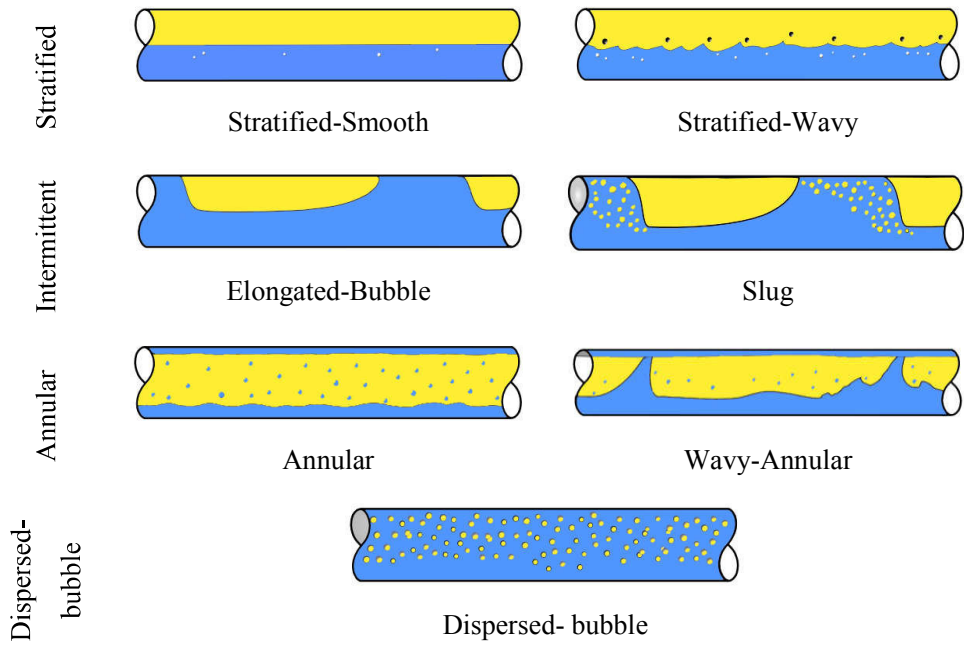
Figure 1.1. Gas-liquid flow patterns in horizontal and near horizontal pipes

(Adapted from [1])

Direction of flow

Bubble

Slug

Churn

Annular

Dispersed-Bubble
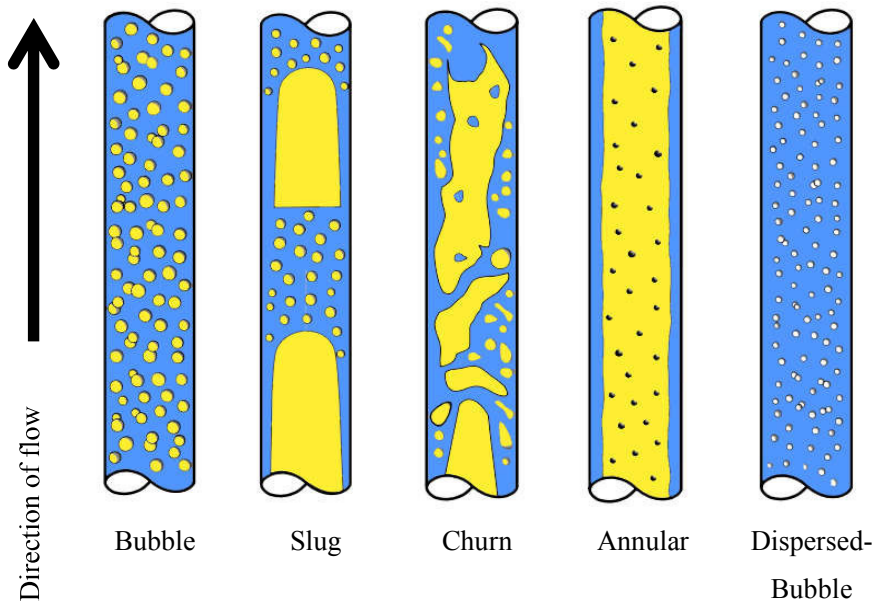
Figure 1.2. Gas-liquid flow patterns in vertical and near vertical pipes

(Adapted from [1])

2

Very long slugs may form in risers in what is often called severe slugging. When a riser is exposed to severe slugging, the density of the internal fluid undergoes large variations since the whole riser can be filled with liquid which blows out at regular intervals. The different stages of the severe slugging cycle in a lazy wave riser are shown in Figure 1.3.

(a)

(b)

(c)

(d)
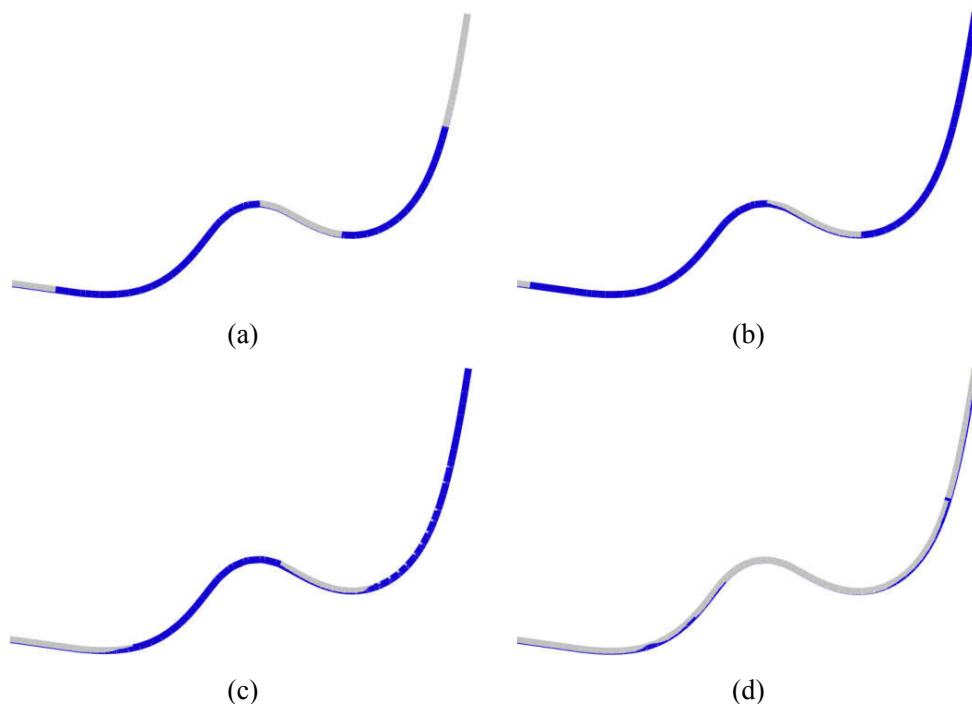
Figure 1.3. Description of severe slugging in a flexible riser. (a) Slug formation, (b) Slug production, (c) Bubble penetration, and (d) Gas blowout.

The change in the internal density, as well as the fluid-wall forces during the violent blowout, can have an effect on the riser geometric configuration. At the same time, a change in geometry can have an important effect on the slugging phenomenon [2].

Since flexible risers in subsea systems can exhibit flow induced movements, structural analysis of flexible pipes should then also involve dynamic simulations of the coupled system. A two-way coupled Fluid-Structure Interaction (FSI) analysis is in some cases needed for gravity dominated flows, where the gas compressibility can give unstable liquid flows. One example is a buoyantly floating pipe. A sag in the pipe can accumulate liquid and lead to further sinking of the pipe with a subsequent blow-out and rise of the pipe again.

Another special case of coupled flow-flexible riser dynamics is the Macondo blowout case. After the explosion and subsequent sinking of the Deepwater Horizon drilling rig in 2010, a section of the collapsed riser partially resting on the seabed showed regular movements. This movement was attributed to variations in the content density induced by slug flow [3]. Other transient operations such as pigging, excursion of hydrate plugs, transient slugs and water hammer can also significant structural impact.

The flow-structure coupling is also important for rigid pipe systems, where high frequency slug flow can induce vibrations. Slug induced forces produce a continuous excitation which can lead to fatigue and pipe failure.

There are commercial simulators for static and dynamic structural analysis of flexible risers. RIFLEX, OrcaFlex and Flexcom are examples of such software. Most of these packages usually include the internal slug flow as simplified slug units, instead of resolving the fluid dynamic equations. General purpose Finite Element Method (FEM) analysis tools, for example, ABAQUS and ANSYS Mechanical have also been used for the analysis of risers and pipelines.

There are also commercial simulators for dynamic multiphase flows in pipes such as OLGA and LedaFlow, where analysis of operational transients (production changes, pigging, shut-in and restarts) and assessment of flow instabilities with propagating liquid slugs are made on fixed geometries. General-purpose Computational Fluid Dynamics (CFD) software like a STAR-CCM+ or ANSYS Fluent might also be used to solve this kind of problems, with the drawback of high computational cost.

A previous study demonstrated a coupling between two separated programs in a case involving a flexible riser conveying slug flow [4]. Currently there is however no stand-alone commercial software capable of simulating two-way interaction in flexible pipes and risers.

The present research aimed to develop and test a computational tool capable of solving the coupled dynamics of flexible pipes conveying multiphase flows. The resulting computational tool should be able to consider geometry variations during the solution of the internal flow dynamics, a as well as predicting the dynamical behavior of the flexible structure due to the internal flow.

1.2 Background

This section provides a literature survey of some studies on two-phase gas-liquid flow interaction with flexible pipes, as well as some studies involving still pipes.

1.2.1 Theoretical studies

Monette and Pettigrew [5] presented a modified fluidelastic instability equation considering two phase flow. The modified equation was based on the equation for cantilever tubes subjected to internal single-phase flow on [6]. Three models for internal flow were studied: homogeneous model, Chisholm's model, and a newly developed model for vertical downward flow. The models were compared with experimental data of a vertical cantilever pipe conveying air-water flow. The dimensionless critical velocity and dimensionless critical frequency were well reproduced by the new model developed by the authors.

An and Su [7] proposed a model for analyzing the dynamic behavior of riser vibration subjected to simultaneous internal gas-liquid two-phase flow and external marine current. They calculated the internal flow variables using the vertical slug flow model presented by [8], and obtained that the amplitude of vibrations increase with the superficial velocities of liquid and gas.

1.2.2 Experimental studies

Das [9] performed a series of experiments on a steel S-shaped riser conveying single phase and two-phase air-water flow. Forces on bends were measured during different stages of the severe slugging cycle. He observed that the resultant dynamic forces on bends were dominated by hydrostatic forces during the build-up and production stages, and relatively larger and fluctuating forces during bubble penetrations and gas blowdown.

Monette and Pettigrew [5] also carried out an experimental study on the fluidelastic instability of vertical cantilever tubes transporting air-water flow. Tubes of different properties and lengths were tested. They observed unstationary instabilities modes where nodes were moving along the tube.

Bordalo, et al. [10] studied the influence of two phase gas-liquid internal flow on a flexible catenary riser through a series of experimental tests on a scaled riser system. The riser was

surrounded by stagnant air so no important external hydrodynamic forces were included. The gas and liquid flow were adjusted to reproduce slug, churn and annular flow patterns. They observed that the movement of the riser increases while increasing the gas flow rate from slug flow to churn-annular transition, and reduces on fully annular flow. They conclude that the internal flow plays a role on the structural dynamic of slender catenary risers.

Da Silva and Bordalo [11] performed an exploratory experimental study of a small scale catenary riser transporting air-water slug flow. They compared the displacement of a point on the riser when the pipe was surrounded by still air or water (positive buoyancy when empty). They observed that the amplitude of pipe displacements induced by slug flow increases as the air flow rate is increased.

Ita [12] designed and ran small-scale experiments consisting of a submerged flexible pipe in catenary and S-riser configuration. The flow patter on study was air-water severe slugging. He reported considerable displacement of the pipe for different stages of the severe slugging cycle.

1.2.3 Numerical studies

The first numerical attempts of including the influence of slug flow in pipes modelled the internal flow as user-imposed density profiles propagating along the pipe at certain velocities. Those studies include the following:

Patel and Seyed [13] introduced a set of equations to describe the behavior of flexible risers with arbitrary geometry exposed to internal and external hydrostatic pressure, forces induced by internal slug flow and external hydrodynamic forces. The density of the internal flow was modelled as a sinusoidal function. They applied a solution technique based on linearized frequency-domain analysis. Agreement was obtained between model predictions and experiments on a case study consisting of a catenary riser supported by both ends. They showed that the effects of dynamic excitation due to momentum change are important in the dynamic response of flexible risers because it can expose the riser to large tension fluctuations, which introduces an additional source of cyclic fatigue loads at the frequency of the slugs. They also showed that the slug induced dynamic excitation can

also produce a dynamic change on the geometric stiffness of the riser due to effective stress variations.

Seyed and Patel [14] showed time domain simulation results of a 510 m long lazy-s riser under waves, vessel motions and slug flow forces. They showed that highly nonlinear loading and riser response might be produced by the combined effects of waves, vessel motions and slug flow, even for low magnitude of wave and vessel induced motions.

Mossa and Pollio [15] employed the lumped mass technique to solve a flexible pipe under constant and variable slug wavelength and period. They modeled the slug wavelength and period as a function of local riser inclination.

Reda, et al. [16] studied the effects of slug flow on a pipeline resting on a sleeper. The analysis was carried out by using the ABAQUS software, where the slug induced loads were included as moving point forces. They compared simulation results considering the combination of slug weight and centrifugal force, and then only slug weight. They concluded that the centrifugal force has little effect when the ratio between maximum centrifugal force and slug weight was less than 10%.

Gundersen, et al. [17] developed a methodology to determine the remnant fatigue life of flexible risers under vessel motion, continuous and regular slug flow and external irregular wave loading. In a test case regarding a lazy-s riser, they demonstrated that the slugging can reduce the riser fatigue life approximately to 50%. The slugging parameters used in the analysis were selected through an iterative process aiming at reproducing riser oscillations observed from different ROV inspections.

Bordalo and Morooka [18] studied the effect of slug flow on a steel catenary riser and a steel lazy wave riser. They carried out a series of simulations using different values of slug frequency and showed its impact on the riser displacement and bending stresses. They concluded that large oscillations may be generated when the slug frequency is close to one of the natural frequencies of the riser.

An interesting study where the fluid dynamic is solved on a moving domain was published by Zaldivar [3]. He carried out a series of simulations involving an oscillating riser conveying internal two-phase flow. Using video footage from Deepwater Horizon riser inspections after the accident took place in 2010, vertical motion of a riser section was identified and characterized, as well as slug frequency at the riser end plume. The observed displacement was imposed as a moving domain in LedaFlow, and different flowrates were

studied with the aim of reproducing the observed slug frequency. Based on this analysis, he was able to estimate the flow rate through the riser.

Other studies solved both the internal fluid flow and structural dynamics. Forces due to the internal flow are applied to the structure but the influence of the structural displacement on the fluid dynamic was neglected. It is worth mentioning:

Nair, et al. [19] presented a combined CFD-FEM analysis of a subsea multi-planar rigid jumper system conveying two-phase oil-gas flow. The flow was solved using a STAR-CCM+ and ABAQUS was used for calculating the structural response. The pressure field on the pipe wall was exported from the CFD software and imposed on the internal wall of the structural domain.

Pontaza and Menon [20] also presented CFD-FEM simulations results of a jumper under slug loads, but in this case, the forces were applied only on flow-turning elements.

Diaz, et al. [21] studied the influence of terrain induced slugging on the dynamic behavior of a pipeline-riser system. The characteristics of the multiphase flow were predicted by using OLGA, and the dynamic response was calculated using FEM. Gravity and momentum forces due to the internal flow were calculated and imposed in the structural model.

Onuoha, et al. [22] studied the influence of pressure fluctuations resulting from severe slugging in the base of a steel riser. They obtained pressure time series from OLGA simulations and imposed those pressures in the internal wall of the riser base section using ABAQUS. Stress and dynamic response was discussed for three different mass flow rates.

Over the past half-decade, an increasing number of researchers have focused their attention on modelling FSI in pipes in a two-way manner. Some of them are mentioned in the following:

Chica, et al. [23] performed coupled 3D CFD-FEM simulations of a steel jumper section using STAR-CCM+ and ABAQUS. The pressure field obtained from the fluid simulation was mapped and imported into the structural simulator. The fluid domain was updated following the predicted displacements. They concluded that the instability of slug flow can induce significant levels of vibration and reduce the fatigue life of the jumper.

Ortega, et al. [4] studied the influence of the slug flow on a lazy wave riser dynamics by exchanging information between two previously independent computer programs. The coupling was made using the High Level Architecture standard to transfer the geometric

configuration from the structural dynamic solver to the 1D multiphase solver, while mass and velocity of each phase were transferred in the reverse direction, so the programs provide two-way feedback dynamically.

Ortega, et al. [24] carried out a study similar to [4] but in this case a non-lineal finite element formulation was employed. They simulated the dynamic response of a catenary riser under the effects of internal hydrodynamic slug flow and external regular waves. The results showed the influence of the external flow on the generation of hydrodynamic slugs because of the change in geometry of the riser, and the amplification of the dynamic response due to the interaction between the external and internal forces.

Jia [25] performed coupled 3D CFD-FEM simulations of a pipeline span, a jumpers and a riser using commercial software. The FSI procedure was implemented by user defined subroutines and build-in functions in both simulators. The slug formation and decay in vibrating pipes could be identified, and the vibration itself was generated by the same multiphase flow phenomenon.

Elyyan, et al. [26] coupled ANSYS Mechanical and ANSYS Fluent for simulating an M shaped jumper. They ran one-way and two-way coupled FSI simulations obtaining that two-way coupled analysis is required to accurately predict pipe deformations during startup conditions, but unnecessary during steady operation conditions.

Lu, et al. [27] also studied the influence of gas liquid flow in a subsea M jumper by means of 3D CFD-FEM simulations using ANSYS Mechanical and ANSYS CFD software. Vortex induced vibrations were also considered in that study. They observed that slug flow induced high-amplitude and low-frequency vibrations, and that the internal production fluids and external seawater contribution to added mass and damping effects can significantly shift the natural frequencies of the jumper.

1.3 Thesis structure

The present thesis is based on a collection of papers. In addition, complementary chapters are included in order to show an extended description of the experimental set-up, processing of results, and to summarize conclusions. An appendix showing a validation study of the selected structural model is also included.

1.3.1 Paper list

The present work has been presented on 6 different scientist publications including both conference papers and journal articles. Each paper contain a different case of study that included the model and qualitatively or/and quantitatively comparison of the numerical prediction and the experimental data generated on the small scale set-up designed on this work.

This section summarizes the research papers produced during this research work. Four papers were presented in national and international conferences, and two manuscripts were submitted to international journals. A different test case is studied in every paper, and experimental results were used for comparing qualitatively or quantitatively the numerical predictions of the coupled model. The papers are presented in chronological order.

- Paper 1: J. Vieiro, A. M. Hemeda and O. J. Nydal. **Multiphase Flow in Flexible Pipes: Coupled Dynamic Simulations and Small Scale Experiments on Garden Hose Instability**. Eighth National Conference on Computational Mechanics, MekIT'15, Trondheim, 18-19 May 2015.

A test case consisting of a flexible hose laid on a smooth surface was presented. A simplified soil contact model was implemented: restrained movement in the vertical direction and Coulomb friction on the horizontal plane. The characteristic oscillatory movement of the pipe due to internal slug flow was reproduced by the simulator. Differences between experiments and simulation results were observed, mainly due to the pipe-soil friction model implemented in the simulator. Imperfections on the hose used in the experiment increased the difficulty in predicting the fluttering period of the hose.

- Paper 2: J. Vieiro, E. I. Ita, O. J. Nydal. **Two-Way Fluid-Structure Interaction in a Flexible Pipe Conveying Gas-Liquid Slug Flow**. OTC Brasil 2015, Rio de Janeiro, 27 - 29 October 2015.

The displacement and internal flow behavior of a flexible pipe in a water tank were studied. Morrison equations were used for modeling the influence of the surrounding fluid on the motion of the pipe. Two hose configurations were considered: the first allowed the hose to float and sink depending on the density of the conveyed mixture, and the second was restricted in a catenary-like shape. The former described a strongly coupled relation

between the flowing fluid and the pipe structure, where large displacements of the pipe were a consequence of accumulation and blow out of liquid.

- Paper 3: J. Vieiro, A. K. Hemeda and O. J. Nydal. **Experimental and Numerical Simulation of Coupled Severe Slugging and Structural Dynamic on a Submerged Flexible Pipe**. International Conference on Advances in Subsea Engineering, Structures & Systems, ASESS 2016. Glasgow, 6-7 June 2016.

On an expert report presented during the Macondo oil spill trial [3], some evidence of coupled fluid and structure periodic behavior was used to estimate the flow rate during some time period. Based on this case, a small scale experimental set up was built and tested. Simulations results of the experimental set up shows a fairly good agreement to the data logged during the experiment. Simulations of a simplified large scale case were also carried out, where it was observed that the periodic motion of the riser was a consequence of liquid accumulation and the liquid accumulation cycle was a consequence of the riser motion.

- Paper 4: J. Vieiro and O. J. Nydal. **Experimental and numerical study of a flexible floating pipe conveying multiphase flow**. Submitted to the Journal of Fluids and Structures.

The article gives a detailed description of the coupled method. As in Paper 2, a floating pipe was studied. The experimental set up was improved and quantitative measurements were used to validate the model predictions. The results showed a strong sensitivity to the pipe diameter and wall thickness, where a few tenths of millimeter may change the behavior of the coupled phenomena.

- Paper 5: J. Vieiro, A. Akhiiartdinov, S. Sævik, C. M. Larsen and O. J. Nydal. **Two-way coupled fluid-structure interaction of a flexible riser conveying slug flow**. Manuscript submitted to Multiphase Science and Technology.

The developed two-way coupled method was used to estimate the dynamic loads on flexible risers. Small scale experiments of a lazy wave riser were used as test cases. Results show significant displacement of the sag bend. The influence of these displacements was negligible on the internal flow dynamic as one-way and two-way coupled simulations predicted practically the same results.

- Paper 6: J. Vieiro, Z. Wang and O. J. Nydal. **Multiphase flow in flexible pipes: simulations and small scale experiments**. 11th North American Conference on Multiphase Technology, Banff, Canada, 6th - 8th June 2018.

A test case consisting of a pig flushing a liquid filled flexible floating hose with attached buoyancy modules was studied. Pressurized air was used to push the pig. Pressure, pig displacement and hose configuration were compared with small scale experiments. Three upstream pressure values were tested. The hose displacements were well reproduced for low and medium air pressure. The hose velocity was overpredicted on the case involving the highest air pressure, possibly due to the simplified model of the hydrodynamic forces on the buoyancy modules.

Chapter 2

Numerical model

2.1 Slug flow and flexible structure interaction

Consider a section of a flexible pipeline conveying multiphase flow as shown in Figure 2.1(a). Due to the multiphysic nature of this problem, it might be divided in two different domains: the first one involving the pipe structure (Figure 2.1(b)) and the second one concerning the fluid dynamics (Figure 2.1(c)). If the behavior of one of the phenomenon does not affect the other, both problems may be studied independently. Otherwise it is necessary to introduce a coupling model between them.

<div align="center">(a)   (b)   (c)</div>
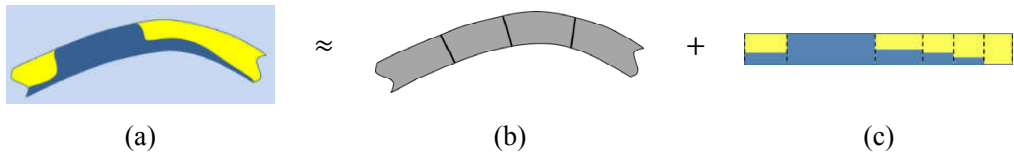
Figure 2.1. (a) Schematic of a flexible pipe conveying gas-liquid flow (b) Structural discretization (c) Fluid domain discretization

This chapter presents a model for considering coupled effect where a lumped mass structural model and a slug tracking multiphase flow model exchange information by means of explicit domain-decomposition [28]. A more detailed description of the model is given in Paper 4.

2.2 Flow model

A 1D hybrid slug capturing and tracking scheme is employed as dynamic multiphase solver for internal flow. The fluid domain is discretized in bubble and slug sections as shown in Figure 2.2. Mass, momentum and energy conservation equations are solved on each section. The domain discretization remains constant when there are not slug sections. If there are slugs present, the mesh is updated following the displacement of each one of

them. This way, the numerical diffusion is reduced. Mesh management is required in order to create, destroy, split or merge elements along the domain. Liquid phase is modelled as incompressible and the gas phase as real gas.
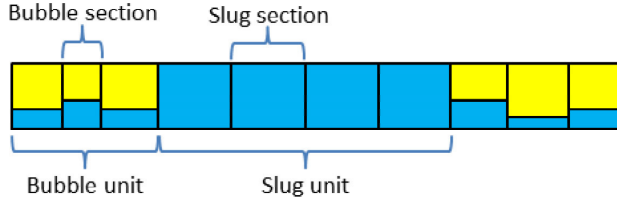
Figure 2.2. Basic discretization of fluid domain.

2.3 Structural model

A model based on lumped mass formulation is selected for solving the structural dynamics. In this model, the pipeline is divided into discrete elements (pipes) with a node on each extreme. For data management reasons, two nodes are used on each element. Consecutive pipes are connected by coupling their nodes, i.e. nodes move together.

The two nodes of a generic pipe L_i are denoted by $S_{i,1}$ and $S_{i,2}$ where sub-indexes 1 and 2 represent upstream node (towards pipe inlet) and downstream node (towards outlet) respectively as shown in Figure 2.3.
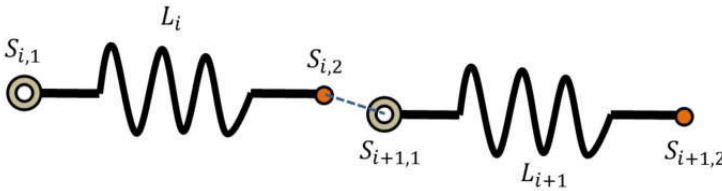
Figure 2.3. Schematics showing both nodes on each element. Coupled nodes $S_{i,2}$ and $S_{i+1,2}$ from consecutive elements shown separated for illustrative purpose.

A general pair of coupled nodes have the form $(S_{i,2}, S_{i+1,1})$. The dynamic equilibrium equations are created for coupled nodes as follows:

$$(m_{i,2} + m_{i+1,1})\ddot{\vec{S}}_{i,j} = \vec{F}_{i,2} + \vec{F}_{i+1,1} \qquad \text{(Eq. 1)}$$

where $m_{i,2} + m_{i+1,1}$ is the mass of the couple and $\vec{F}_{i,2} + \vec{F}_{i+1,1}$ includes all relevant external and internal forces.

2.4 Coupling

Since the fluid mesh is independent of the structural mesh, a coupling step is required for mapping variables from one domain into the other. Figure 2.4 shows an example where a slug section extends across two structural elements.

Figure 2.4. Example where fluid and structural discretization do not match

The mass is distributed according to the length of the section overlapping the pipe. In case of diameter change, a relation based on volumes is required.

In general, the mass m of a phase ϕ in pipe L_i is given by:

$$^{\phi}m_i = \sum_{k=1}^{n} {}^{\phi}m_k \frac{\lambda_{k\cap i}A_i^i}{V_k} \qquad \text{(Eq. 2)}$$

where $\lambda_{k\cap i}$ is the length of fluid section k within the pipe i, A is the cross-sectional inside area of a pipe and V_k is the volume of fluid section k. Other variables like pressure p, volume fraction $^{\phi}\alpha$, phase velocity $^{\phi}U$ or wall wetted perimeter $^{\phi}S$ are calculated using weighted average:

$$\Gamma_i = \frac{1}{|\vec{L}_i|} \sum_{k=1}^{n} \gamma_k \lambda_{k\cap i} \qquad \text{(Eq. 3)}$$

where γ_k represents the variable to be mapped in fluid section k, and Γ_i is the same property mapped on structural element i.

Due to the different time scales on the structural and fluid models, time discretization may differ for the two phenomena. Certain time instants for feedback have to be set. It was stablished that the coupling was going to be carried at out every fluid time step, and the structural time step was set in order to reach those same instants as shown in Figure 2.5.
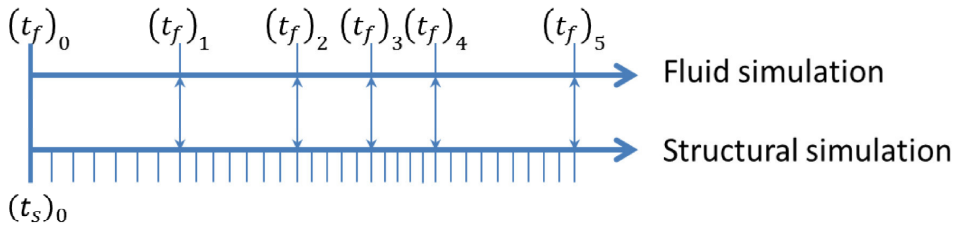
Figure 2.5. Example of fluid and structural time discretization

The information transferred during the coupling stage consists of pipe inclinations (β_i) from the structural solver to the fluid solver, while volume fraction (α_k), velocity (v_k), mass (m_k), wall wetted perimeter (s_k), and mass flow rate ($\dot{m}_k$) of each phase ϕ is transferred in the opposite direction as shown in Figure 2.6.
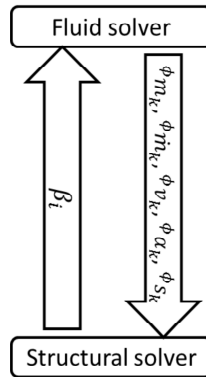
Figure 2.6. Data Exchange during the simulation

Figure 2.7 presents a simplified flowchart for the coupled simulations. The data exchange and domain translation is showed as a bidirectional arrow at the bottom left corner. More details about the model and implementation are presented in Paper 4.
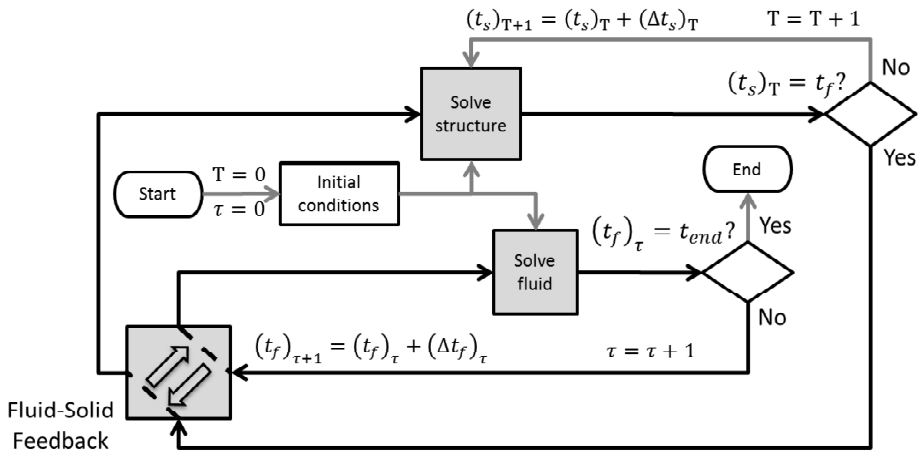
Figure 2.7. Simplified algorithm for fluid-structure coupled simulation

Chapter 3

Experimental setup

This chapter focuses on describing the equipment used during the experimental work as well as describing the experimental procedures and analysis of the experimental results.

3.1 Equipment

3.1.1 Mini-loop

The mini-loop is a box containing a pump, compressor, separator, pressure sensor and flow meters. It was designed to be a portable laboratory capable of producing small scale experiments of two phase air-water flow. It has been upgraded along the years following the needs of several master projects [12, 29, 30]. Pictures of the mini-loop are shown in Figure 3.1 and Figure 3.2. Figure 3.3 shows a diagram of the piping and instrumentation in the mini-loop and its connections to the test section.

Figure 3.1. Front view of the mini-loop
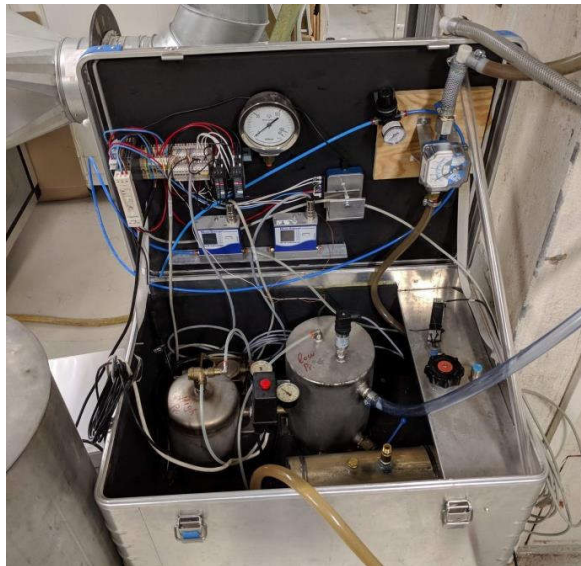
Figure 3.2. Top view of the mini-loop.
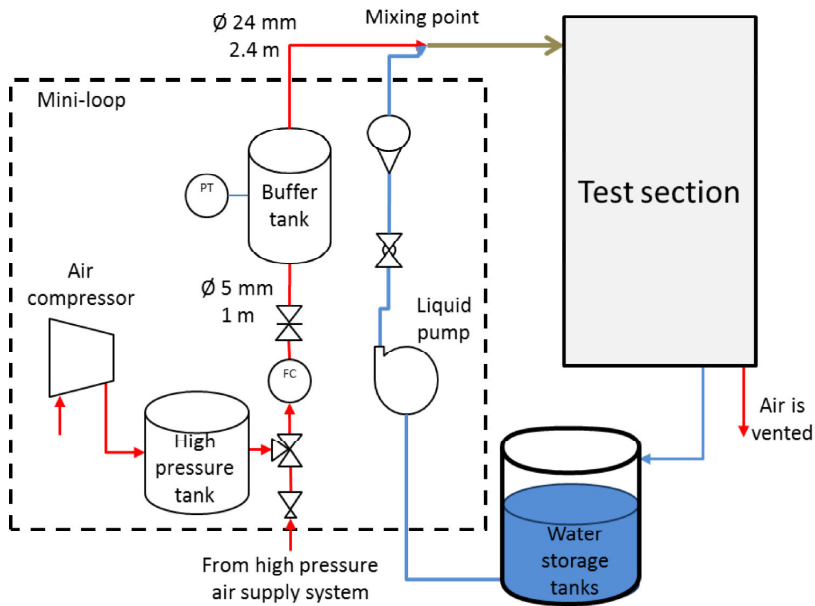
Figure 3.3. Schematics of the main components in the mini-loop.

A list of the present components of the mini-loop is contained in Table 3.1.

Table 3.1. Main components of the mini-loop.

Water pump	GRUNDFOS UPS 25-40 180
Air compressor	DING HWA AC 100
Water flow meter	Tecfluid M21160
Air mass flow meter & controller	Mass-Stream D-6341-D-DR
Pressure transducer	Druck PTX 1400
Data acquisition device	National instruments USB-6001

The air flowrate supplied by the compressor in the mini-loop was too small for some of the experiments. Thus an 8 bar air supply line was used instead for experiments in papers 4, 5 and 6. A pressure regulator was used to reduce the inlet pressure to 1 bar.

3.1.2 Flexible hoses and accessories

Flexible hoses of different diameters were used as test sections for fluid-structure interaction experiments. The characteristics of those hoses are presented in Table 3.2.

Table 3.2. Properties of flexible hoses

	Hose 1	Hose 2	Hose 3
External diameter (mm)	9	16	21.8
Internal diameter (mm)	6	12	15
Wall thickness (mm)	1.5	2	3.4
Linear mass density (kg/m)	0.044	0.118	0.230
Elastic modulus (MPa)	14.1	5.0	2.5

Red adhesive tapes were set to some points along the hose in order to improve visibility for tracking purposes.

Buoyancy and ballast were needed for obtaining s-riser configurations. The buoyancy sections were made of flexible polyethylene foam for pipe isolation applications, while ballast was included by attaching a stainless steel chain to the hose.

For experiments involving pigging operations, rubber water balloons were used as "pigs". The balloons were filled with approximately 5 cm^3 of water for running pigging experiments in Hose 3.

3.1.3 Water tanks

Three water tanks were used during different experiments. The dimensions of those tanks are given in Table 3.3. Only Tank 3 has a glass wall for visual access as shown in Figure 3.4. Underwater cameras were used in Tank 1 and Tank 2.

Table 3.3. Dimensions of the water tanks

	Tank 1	Tank 2	Tank 3
Length (m)	35	0.95	4
Wide (m)	3.5	0.95	0.5
Depth (m)	1.6	0.4	1.5

Figure 3.4. Picture of tank 3.

Tank 1 and Tank 2 were used during the experimental campaigns for Paper 2 and Paper 3 respectively. Tank 3 was used for Papers 4, 5 and 6.

3.1.4 Video cameras

Three video cameras were employed in this research, only one of them was used in a given experimental campaign. The cameras were set to the resolution and frame rate values in Table 3.4 during video recording.

Table 3.4. Model and configuration of employed video cameras.

	Camera 1	Camera 2	Camera 3
Model	GoPro Hero4 Black	Canon EOS60D	Sony HXR-MC200E
Resolution	1920x1080	1920x1080	1920x1080
Frame rate	30	25	100

Camera 1 was used for underwater recording (Paper 2 and Paper 3) and Camera 3 for pigging experiments (Paper 6). Camera 2 was used in the rest of the experiments. The recorded videos were processed using the algorithm in section 3.2.2.

3.1.5 Load sensors

In order to record top tension fluctuations in the lazy wave riser case, a Tedea-Huntleigh 1022M-3M-F-106 load sensor was installed. The sensor was capable of measuring up to 30 N. The signal form the load cell was conditioned using a Status Instruments SEM1600B and then sent to the data acquisition device in the mini-loop.

3.2 Data acquisition and analysis of experimental results

LabVIEW™ and MATLAB® were used for data acquisition and processing respectively. A short description of the programs is given in the following.

3.2.1 Data acquisition software

A LabVIEW program was generated for sending and receiving data from the data acquisition device and Camera 2. The program shows graphically readings from sensors as well as previews images from the video camera. Logging and video recording were also possible through this application. Figure 3.5 shows a screen capture of the data acquisition software.
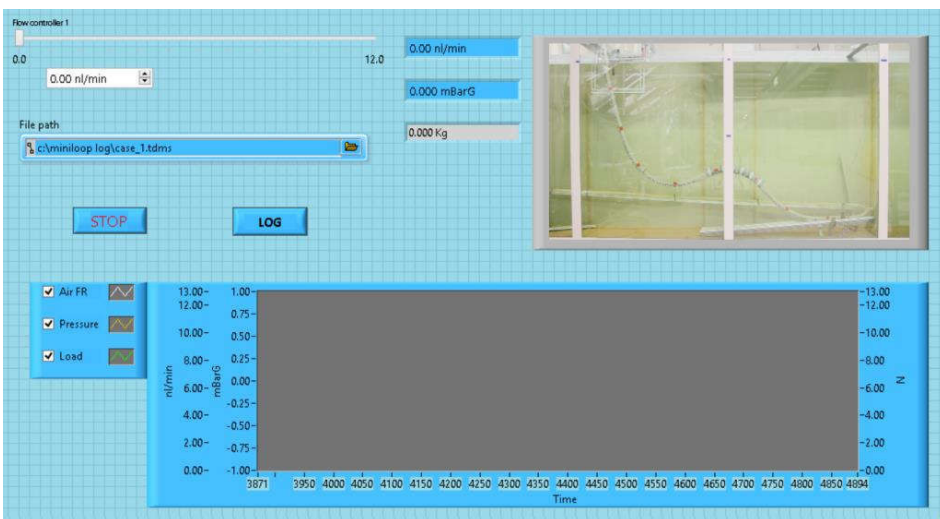
Figure 3.5. Screen capture of data acquisition software.

3.2.2 Video processing

In order to extract the coordinates of the points of interest along the hose, a MATLAB script base on the code of [29] was written. The code makes use of MATLAB's Image Processing Toolbox™ for image manipulation and analysis. The basic steps for processing each frame in a video file are:

- Create new image with the red layer of the original RGB frame.
- Convert the original RGB frame into grayscale.
- Subtract the grayscale image form the red layer image.
- Apply a 2-D median filter.
- Convert into binary image.
- Calculate the coordinates (in pixels) of the centroid for each connected components.

Other tasks such as removing reflected marks on the water surface and recovering marks behind tank beams were also performed. After a video file was completed processed, the pixel coordinated were converted into meters taking into account refraction due to the tank glass wall and water.
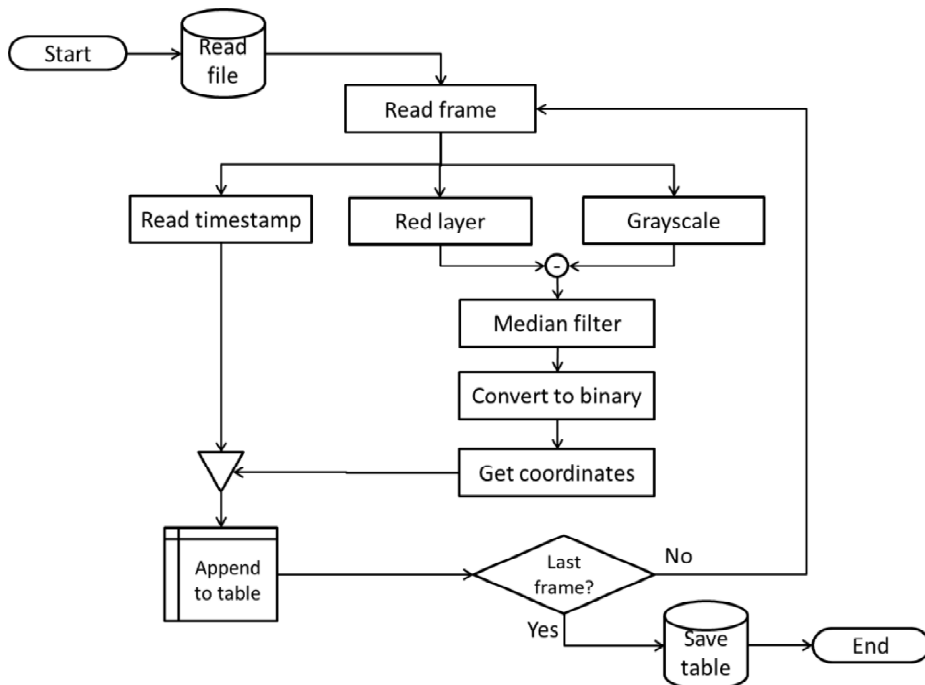
Figure 3.6. Video processing flowchart.

Figure 3.7 shows images from different stages during the image processing procedure for the lazy wave riser case. Complement images (black and white are reversed) are shown in Figure 3.7(d), (e) and (f) in order to ease visualization of the marks.
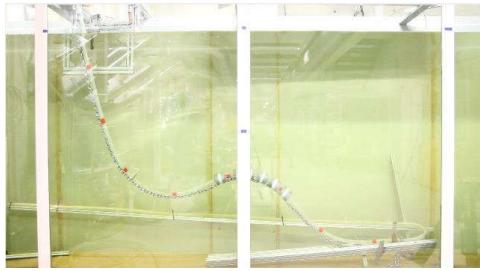
(a) Original RGB image
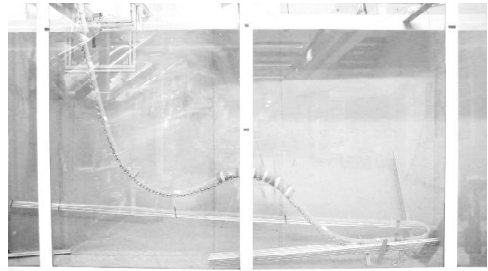
(b) Red layer
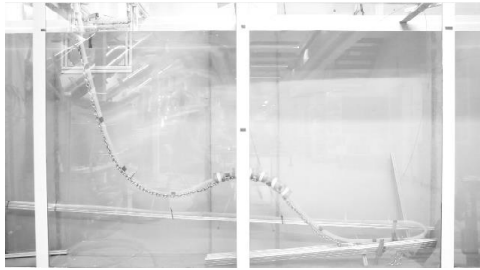
(c) Grayscale

(d) Red layer minus grayscale (Complement)

(e) After mean filter (Complement)

(f) Binary image (Complement)
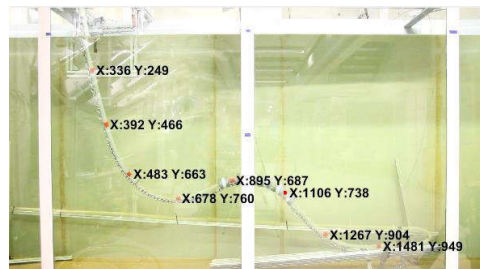
(f) Coordinates of located marks (in pixels)

Figure 3.7. Images from different stages of image processing algorithm

Chapter 4

Conclusions and further work

4.1 Conclusions

This research focused on studying the fluid-structure interaction on flexible pipes conveying multiphase flow. This was achieved by incorporating a structural dynamic model into an existent multiphase flow dynamic software. An explicit domain-decomposition method was employed to solve the system. The resulting computer program was able of predicting the internal multiphase flow dynamic and pipe displacements including coupled effects.

Different test cases involving diverse degrees of fluid-structure coupling were studied, including garden hose instability, a floating hose and a lazy wave riser. All the cases were studied both experimentally and numerically. The displacement of certain points along the flexible domain and upstream pressure were used as main parameters for comparing simulation results and experimental measurements. Even though all the studied test cases were based on small scale and low pressure setups, valuable information was obtained.

The fluttering observed during the garden hose experiments was reproduced with the model. An improved pipe-soil model is required in order to obtain a better prediction of the pipe dynamics.

Stronger fluid-structure coupling was observed in the cases where the inlet and outlet of a flexible submerged test section were at the same level (floating pipe and submerged bend pipe). A weaker coupling was observed in the lazy wave riser case, where two-way coupled simulations were unnecessary, as the flow pattern was not considerably influenced by the movements of the buoyancy section.

Despite the simplicity of the selected structural model, fairly well predictions were obtained in terms of both structural behavior and internal flow characteristics.

4.2 Suggestions for further work

Previous researches have shown numerically that the slug flow effects might amplify the dynamic response of a riser subjected to vessel motion and waves. A validation study of a flexible riser under these conditions is suggested.

Other test cases involving displacement of floating production units, waves or total pipe rupture may provide interesting information about the coupled phenomena. Validation against large scale and high pressure cases is also necessary.

The simulation time might be considerably reduced by using an implicit time integration method in the structural dynamic solver. In this case, the researcher should verify that predictions of the coupled physics are not harm by larger structural time steps.

From the floating hose case, it was observed that small differences deviations in the pipe diameter may have important effects on the coupled dynamic. Considering deformations on the pipe wall cross section due to pressure difference or ovalization due to bending may improve the quality of the results.

As described in the literature review, increasing attention has been focused on the influence of slug flow in subsea jumpers. The structural model will need some improvements in order to accurately describe the dynamics on pipe bends in this kind of structures.

References

[1]   O. Shoham, *Mechanistic Modeling of Gas-Liquid Two-Phase Flow in Pipes*: Society of Petroleum Engineers, 2006.

[2]   A. Moros and P. Fairhurst, "Production riser design: Integrated approach to flow, mechanical issues," *Offshore Magazine,* vol. 59, 1999.

[3]   M. Zaldivar, "Quantification of Flow rate during slug flow," 2013.

[4]   A. Ortega, A. Rivera, O. J. Nydal, and C. M. Larsen, "On the Dynamic Response of Flexible Risers Caused by Internal Slug Flow," presented at the 31st International Conference on Ocean, Offshore and Arctic Engineering, Rio de Janeiro, Brazil, 2012.

[5]   C. Monette and M. J. Pettigrew, "Fluidelastic instability of flexible tubes subjected to two-phase internal flow," *Journal of Fluids and Structures,* vol. 19, pp. 943-956, 2004.

[6]   M. P. Paidoussis, *Fluid–Structure Interactions: Slender Structures and Axial Flow* vol. 1. London: Academic Press, 1998.

[7]   C. An and J. Su, "Vibration Behavior of Marine Risers Conveying Gas-Liquid Two-Phase Flow," 2015.

[8]   Y. Taitel, "Stability of severe slugging," *International Journal of Multiphase Flow,* vol. 12, pp. 203-217, 1986.

[9]   I. A. F. Das, "The Characteristics and Forces due to Slugs in an 'S' Shaped Riser," PhD Thesis, School of Engineering, Cranfield University, 2003.

[10]   S. N. Bordalo, C. K. Morooka, C. C. P. Cavalcante, C. G. C. Matt, and R. Franciss, "Whipping Phenomenon Caused by the Internal Flow Momentum on the Catenary Risers of Offshore Petroleum Fields," presented at the ASME 2008 27th International Conference on Offshore Mechanics and Arctic Engineering, Estoril, Portugal, 2008.

[11]   Z. Da Silva and S. N. Bordalo, "Experimental set up to study the oscillation induced by two-phase flow in small scale models of production risers for offshore petroleum fields," presented at the 22nd International Congress of Mechanical Engineering (COBEM 2013), Ribeirão Preto, SP, Brazil, 2013.

[12]   E. I. Ita, "Small scale experiments on severe slugging in flexible risers," Department of Energy and Process Technology, Norwegian University of Science and Technology, 2011.

[13]   M. H. Patel and F. B. Seyed, "Internal flow-induced behaviour of flexible risers," *Engineering Structures,* vol. 11, pp. 266-280, 1989.

[14]   F. B. Seyed and M. H. Patel, "Considerations In Design Of Flexible Riser Systems," presented at the The Second International Offshore and Polar Engineering Conference, San Francisco, California, USA, 1992.

[15]   M. Mossa and A. Pollio, "Flexible pipe behaviour investigation using two models of internal slug flow regime," presented at the The 9th International Symposium on Fluid Control, Measurement and Visualization (FLUCOME 2007) Tallahassee, Florida, 2007.

[16]   A. M. Reda, G. L. Forbes, and I. A. Sultan, "Characterisation of Slug Flow Conditions in Pipelines for Fatigue Analysis," pp. 535-547, 2011.

[17] P. Gundersen, K. Doynov, T. Andersen, and R. Haakonsen, "Methodology for Determining Remnant Fatigue Life of Flexible Risers Subjected to Slugging and Irregular Waves," presented at the 31st International Conference on Ocean, Offshore and Arctic Engineering, Rio de Janeiro, Brazil, 2012.

[18] S. N. Bordalo and C. K. Morooka, "Slug flow induced oscillations on subsea petroleum pipelines," *Journal of Petroleum Science and Engineering,* vol. 165, pp. 535-549, 2018.

[19] A. Nair, C. Chauvet, A. Whooley, A. Eltaher, and P. Jukes, "Flow Induced Forces on Multi-Planar Rigid Jumper Systems," pp. 687-692, 2011.

[20] J. P. Pontaza and R. G. Menon, "Flow-Induced Vibrations of Subsea Jumpers due to Internal Multi-Phase Flow," pp. 585-595, 2011.

[21] M. J. C. Diaz, D. Gonzalez, A. Parra, E. Casanova, and M. Asuaje, "Effect of Gas-Liquid Two Phase Flow in the Structural Behavior of Pipelines " presented at the 8th International Conference on Multiphase Flow ICMF 2013, Jeju, Korea, 2013.

[22] M. D. U. Onuoha, Q. Li, M. Duan, and Q. Gao, "Severe slugging in deepwater risers: A coupled numerical technique for design optimisation," *Ocean Engineering,* vol. 152, pp. 234-248, 2018.

[23] L. Chica, R. Pascali, P. Jukes, B. Ozturk, M. Gamino, and K. Smith, "Detailed FSI Analysis Methodology for Subsea Piping Components," presented at the ASME 2012 31st International Conference on Ocean, Offshore and Arctic Engineering, Rio de Janeiro, Brazil, 2012.

[24] A. Ortega, A. Rivera, and C. M. Larsen, "Flexible Riser Response Induced by Combined Slug Flow and Wave Loads," presented at the ASME 2013 32nd International Conference on Ocean, Offshore and Arctic Engineering, Nantes, France, 2013.

[25] D. Jia, "Slug Flow Induced Vibration in a Pipeline Span, a Jumper and a Riser Section," presented at the Offshore Technology Conference, Houston, Texas, USA, 2012.

[26] M. A. Elyyan, Y. Y. Perng, and M. Doan, "Fluid-Structure Interaction Modeling of a Subsea Jumper Pipe," presented at the ASME 2014 33rd International Conference on Ocean, Offshore and Arctic Engineering, San Francisco, California, USA, 2014.

[27] Y. Lu, C. Liang, J. J. Manzano-Ruiz, K. Janardhanan, and Y.-Y. Perng, "Flow-Induced Vibration in Subsea Jumper Subject to Downstream Slug and Ocean Current," *Journal of Offshore Mechanics and Arctic Engineering,* vol. 138, pp. 021302-021302-10, 2016.

[28] S. K. Chimakurthi, S. Reuss, and W. Shyy, "Fluid-Structure Interactions," in *Handbook of Fluid Dynamics*, R. Johnson, Ed., Second Edition ed Boca Raton: CRC Press, 2016, pp. 31-1-31-24.

[29] A. K. Hemeda, "Structure-Slug Flow Coupling: Small Scale Experiments with Submerged Flexible Pipes," Master thesis, Department of Energy and Process Engineering, NTNU, 2015.

[30] A. Akhiiartdinov, "Small Scale Experiments with Gas-Liquid Slug Flow in Floating Pipes," Master thesis, Department of Energy and Process Engineering, NTNU, 2016.

[31] C. M. Larsen, "Flexible riser analysis - comparison of results from computer programs," *Marine Structures,* vol. 5, pp. 103-119, 1992.

Apendix A.

Validation study of structural dynamic model

This appendix presents a validation study of the structural dynamic model. The selected test cases were taken from the well-known benchmark test presented by Larsen [31]. It consists of a flexible lazy wave riser under different static and dynamic hydrodynamic loads and vessel motion. Results from 11 different software are reported on [31] as well as statistical data in term of mean data and standard deviations. Mean values on [31] are used here as reference.

The riser was discretized into 116 elements from 2 to 10 meters long. Details of the structural mesh are shown on Figure A.1. The time integration was done using the explicit Euler-forward method. The time step was set to 0.001 s for all the simulations.
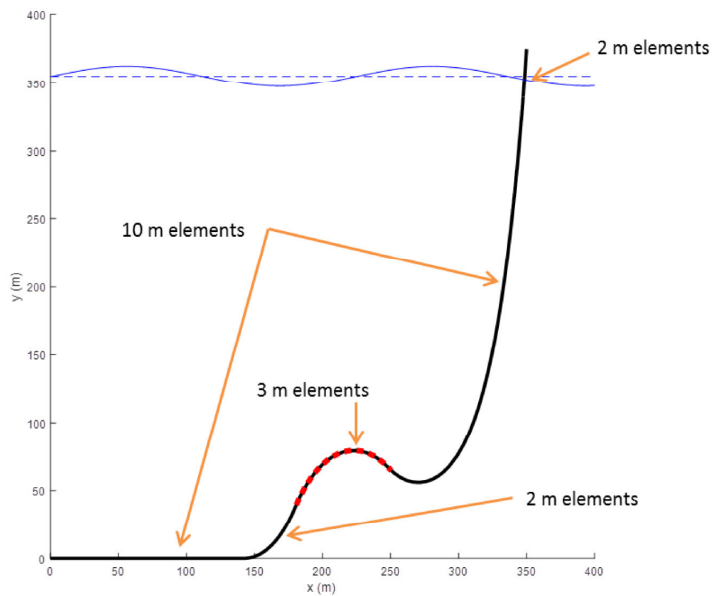
Figure A.1. Structural mesh details

Static analysis

Three of the four cases considering static forces on [31] were simulated.

Case 1 – Still water

An arbitrary initial condition was given and the dynamic equations were integrated over time until no significant variations were observed. The static geometry is presented in Figure A.2. This static geometry was given as initial condition for all the other simulated cases in order to reduce simulation time. Table A.1 compares the obtained results and the reported on the benchmark study.

Table A.1. Results comparison for still water simulation

	Top tension	Bottom end tension	TDP x	Local maximum x	Local maximum y	Curvature
	(kN)	(kN)	(m)	(m)	(m)	(m^{-1})
This study	177.8	11.9	142.3	218.9	79.10	0.0351
Larsen [31]	176.8	19.0	140.0	225.1	79.34	0.0357

Case 2 – Static in-plane current

A second simulation, now with constant current velocity was carried out. Results are shown on Table A.2 and Figure A.2. It is observed that the bottom end tension differs from the reference value, but it is still inside reported the standard deviation.

Table A.2. Results comparison for static in-plane current

	Top tension (kN)	Bottom end tension (kN)	TDP x (m)	Local maximum x (m)	Local maximum y (m)	Local maximum Curvature (m^{-1})
This study	173.6	7.3	144.2	207.1	87.35	0.04846
Larsen [31]	173.7	16.0	142.0	209.2	88.24	0.04985
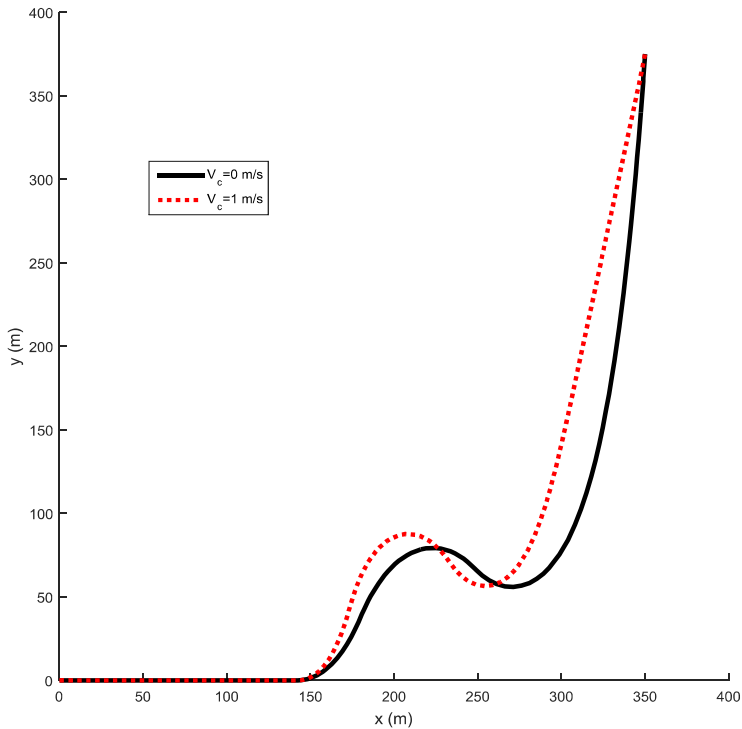
Figure A.2. Static configuration for still water and in-plane current

Case 3 – Static out-of-plane current

In this case, a constant current velocity of 1 m/s in the z direction was set. The coordinates of the local minimum and local maximum as well as tension on those points were studied. Results are presented in Table A.3 and Table A.4. The static geometry of the riser is plotted in Figure A.3.

Table A.3. Results comparison for static out-of-plane current, local minimum

	x (m)	y (m)	z (m)	Tension (kN)
This study	269.73	58.04	29.18	12.73
Larsen [31]	263.6	61.8	29.56	13.48

Table A.4. Results comparison for static out-of-plane current, local maximum

	x (m)	y (m)	z (m)	Tension (kN)
This study	222.7	79.18	27.7	12.63
Larsen [31]	222.5	77.55	25.7	13.56
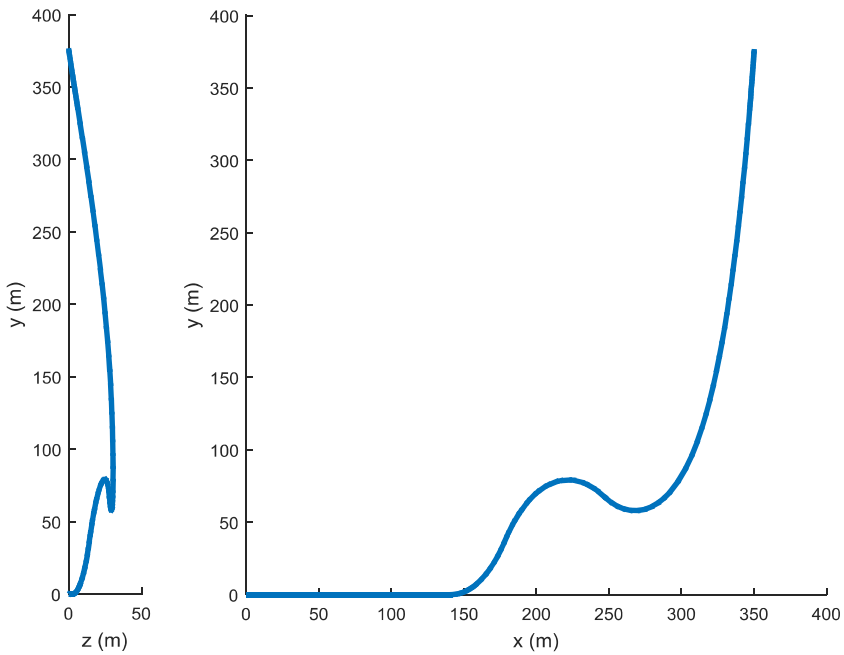
Figure A.3. Static configuration out-of-plane current

The values calculated for this case were fairly close to the reference values.

Dynamic analysis

All the dynamic cases presented on [31] were reproduced here. The results were as follows.

Case 5 – Regular wave and in-plane current

Dynamic forces due to waves were included in the total force. The sea surface was modeled as smooth and horizontal, so the buoyancy force was constant over time for any point in space. Table A.5 shows the maximum and minimum dynamic top tension and the difference between them.

Table A.5. Dynamic top tension for wave and in-plane current

	max (kN)	min (kN)	ΔT (kN)
This study	172.5	167.3	5.2
Larsen [31]	182.7	166.3	16.4

The maximum top tension was underestimated. This may be a consequence of neglecting the normal drag force. Figure A.4 displays some riser geometries during the simulation.
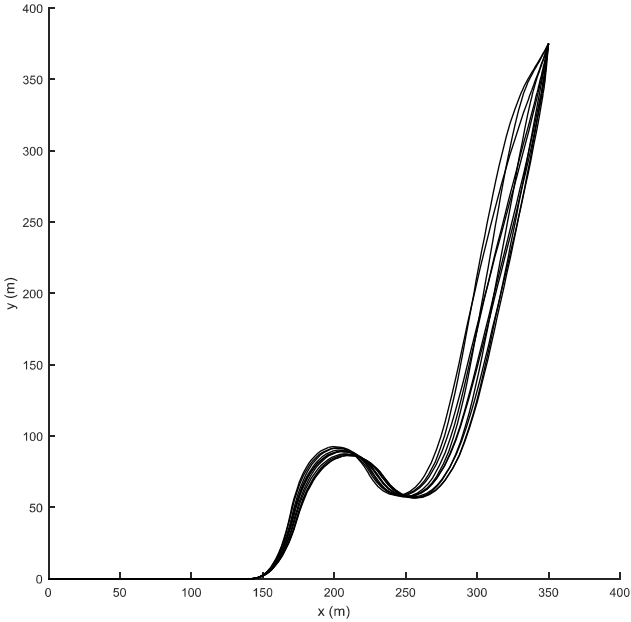
Figure A.4. Riser geometry for different times (Case 5)

Case 6 – Top end motion, regular waves and in-plane current

In this case, an elliptic vessel motion was set along with the same waves and current of the previous case. The dynamic top tension is displayed in Table A.6. Better results were obtained in this case than in the previous one. Figure A.5 shows the riser geometry for different times.

Table A.6. Dynamic top tension for wave, in-plane current and vessel motion

	max (kN)	min (kN)	ΔT (kN)
This study	243.9	111.0	132.9
Larsen [31]	248.8	105.6	143.2
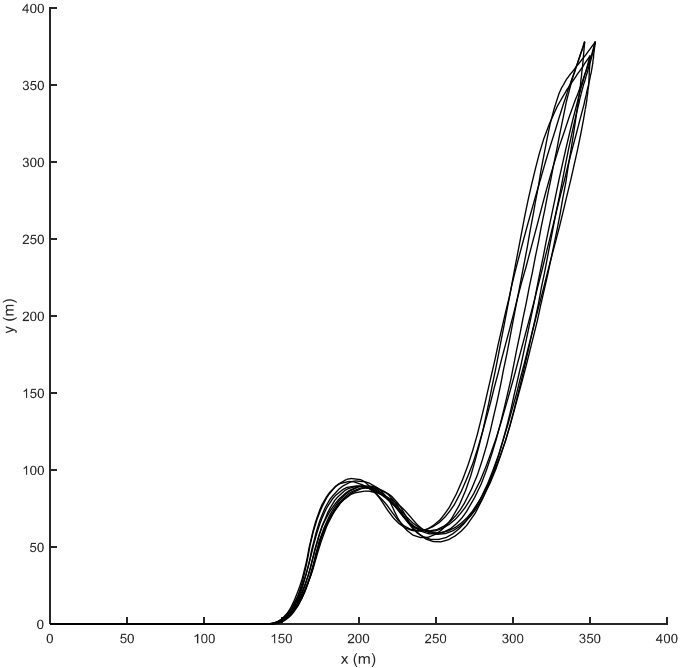
Figure A.5. Riser geometry for different times (Case 6)

Paper 1 - Multiphase flow in flexible pipes - Coupled Dynamic Simulations and Small Scale experiments on Garden Hose Instability

MULTIPHASE FLOW IN FLEXIBLE PIPES: COUPLED DYNAMIC SIMULATIONS AND SMALL SCALE EXPERIMENTS ON GARDEN HOSE INSTABILITY

JOAQUIN J. VIEIRO, AMR M. HEMEDA AND OLE J. NYDAL

Department of Energy and Process Engineering
Norwegian University of Science and Technology (NTNU)
Kolbjørn Hejes v 1B, NO-7491 Trondheim, Norway
e-mail: joaquin.vieiro.medina@ntnu.no, www.ntnu.edu/ept

Key words: Fluid-structure interaction, two-phase flow, flexible pipes, garden hose instability

Abstract. The garden hose instability is a characteristic phenomenon of fluidelastic instability on flexible pipes conveying fluids. It consists in pipe fluttering due to internal flow induced forces on the pipe wall. In order to study this phenomenon, some small scale experiments of water and air-water two-phase flow through an open ended flexible pipe were carried out. The experiments are compared with numerical simulations using a coupled flow and structure model. The model solves both multiphase flow and structure dynamics in the time domain. The dynamics of an open ended pipe is reproduced in the simulations.

1 INTRODUCTION

Flexible pipes are often used in offshore oil and gas production systems to transport the well fluids from the seabed to surface facilities. These flexible pipes are exposed to multiple external loads like sea current drag, vortex shedding induced forces, waves and seabed interaction as well as internal fluid loads. Under certain conditions, the produced gas and liquid may exhibit intermittent liquid and gas flow (slug flow), potentially causing large variation in pipe tension and large motion due to the internal flow dynamics [1].

Two-way fluid-structure interaction simulations on flexible risers have been demonstrated by Ortega *et al*. [2, 3], reporting important effects of slug flow on the structural dynamic but without comparisons with experimental or full scale field data.

Due to the lack of full scale measurements of the impact of internal multiphase flow in pipeline-riser systems, a small scale experiment has been designed in the NTNU Multiphase Flow Laboratory. The experiment involves fluidelastic instabilities as the one observed in a garden or fire hose which is left free over a smooth surface.

2 NUMERICAL MODEL

In this section the main features of the internal fluid flow simulator as well as the basic equations of the structural dynamic model are presented. Finally, the coupling procedure of the two models is described.

2.1 Fluid dynamics

The internal flow is solved using a one-dimensional two-fluid model based on a slug tracking model formulation [4]. A dynamic mesh describes the bubbles and slugs regions and each of these regions can have a subgrid (sections) as shown in Figure 1.
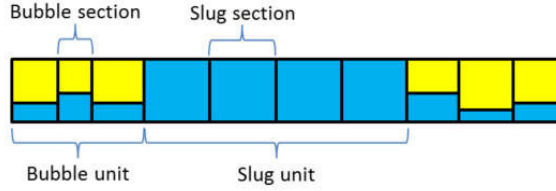

Figure 1: Mesh elements in the slug tracking scheme

The slug units are solved as incompressible fluid and the gas units as compressible using the two fluid model [4], i.e. mass, momentum and energy equations are solved for each phase. The mass equations give the phase fractions. A state equation is required for the gas region. The liquid slug formation can be captured directly from the two-fluid model on a stationary grid, and the slugs and bubbles are tracked thereafter with a moving grid.

The general mass conservation equation for a fluid phase k is expressed by:

$$\frac{\partial \alpha_k \rho_k}{\partial t} + \frac{\partial (\alpha_k \rho_k U_k)}{\partial \Lambda} = \Psi_k \qquad (1)$$

where α is the volume fraction, ρ is the density, U is the average cross-sectional velocity, Ψ is the mass transfer terms, t is the time and Λ is the pipe longitudinal axis coordinate. The momentum equation for a phase k is given by:

$$\frac{\partial (\alpha_k \rho_k U_k)}{\partial t} + \frac{\partial (\alpha_k \rho_k U_k^2)}{\partial \Lambda} = -\alpha_k \frac{\partial p}{\partial \Lambda} - F_{wall,k} \pm F_{int,k} - G_k \qquad (2)$$

where p is the pressure field, $F_{wall,k}$ is the friction force between phase k and the pipe wall, $F_{int,k}$ is the friction force between phase k and its interphase with another phase, and G is the gravity force, including a term to take into account a level gradient force. Details about extension of these conservation equations to the slug tracking framework can be found in [5].

2.2 Structural dynamics

The model presented here is based on the lumped mass method shown by Ghadimi [6] and extended to consider structural damping and internal flow forces. The pipeline is divided into

an arbitrary number of elements, connected in sequence by their nodes. The mass of each element and the fluids contained in it are lumped equally on the two nodes at which it is connected to. The node position $\vec{s}$, velocity $\vec{v}$, and acceleration $\vec{a}$ relative to a stationary coordinate system are defined with three dimensional vectors as follows:

$$\vec{s}_i = \begin{Bmatrix} x_i \\ y_i \\ z_i \end{Bmatrix} \qquad \vec{v}_i = \dot{\vec{s}}_i \qquad \vec{a}_i = \dot{\vec{v}}_i \qquad\qquad (3)$$

where subscript i represents the node number. The pipe structural properties (stiffness and damping) are modeled as massless springs and dampers as shown on Figure 2.
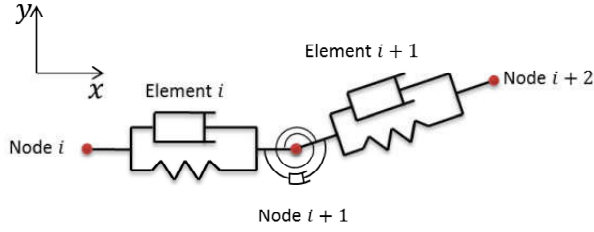

Figure 2: Schematic representation of the mechanical system

The dynamic equilibrium equation for each node is as follows:

$$m_i \vec{a}_i = \vec{F}_i \qquad\qquad (4)$$

Here, m_i represents the lumped mass on node i. $\vec{F}_i$ includes representative forces, in this case: internal structure forces (stiffness and damping), gravity, soil friction, internal fluid friction and centrifugal forces due to fluid momentum variation. Since fluid and structural meshes are not necessarily equal, it is required to convert some of the calculated fluid fields (phase velocities, volume fraction and pressure) from the fluid sections into the structural elements based on overlapping length fraction and volume fraction on fluid sections.

The contribution of internal flow to damping [7] is not included in this model. There is no backward reaction force due to ejected fluid as explained by [8]. Time integration of Equation 4 is performed by Newmark beta method [9].

2.3 Fluid-structure coupling

The fluid-structure coupling is done as follows:

- The fluid equations are solved and the fluid mesh is updated. All fluid parameters are updated on each fluid cell.
- Calculate fluid fields on each structural element.
- The fluid-wall friction force is obtained from the fluid dynamics solver and the centrifugal force on the pipe wall is calculated as the variation of the momentum across nodes for each fluid phase.
- The total force $\vec{F}_i$ is updated and the structural equations are solved. The system geometry is updated according to the calculated displacements.
- Move one time step forward and repeat the calculation steps above until final time is reached.

3 TEST CASE

In order to validate the coupled fluid-structure interaction model, a small-scale experiment was selected. The test consisted on a flexible hose laid on a smooth horizontal surface conveying air-water flow. Details about the experimental setup and simulation configuration are given in the following sections.

3.1 Experimental setup

The experiments have been carried out using a silicon hose of 6 mm internal diameter and 9 mm external diameter. Air and water were supplied using an air compressor and centrifugal pump. The two fluids are mixed in a symmetric "Y" fitting. One end of the hose was clamped and the other one was free to move. The hose was laid over a smooth acrylic sheet covered with a soap-water mixture in order to reduce friction. Figure 3 shows a schematic diagram of the experimental apparatus used for the experiment.
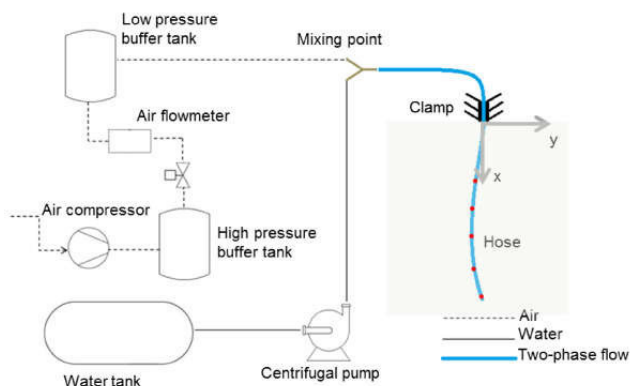
Figure 3: Experimental assembly

The air and water mass flow rates were set to 0.24 g/s and 16.52 g/s respectively (liquid and gas superficial velocities of 0.58 m/s and 6.78 m/s). Fluttering was obtained under these conditions. The movement of the hose was recorded by using a digital camera. Three frames are shown in Figure 4. A tracking algoritm was applied to the video in order to obtain the position of five prestablised points on the hose (Figure 5). The displacement of those five points over the horizontal plane with origin on the clamped point are plotted on Figure 6. From video analysis it was also possible to obtain a slug frequency of approximately 3.3 slugs per second.

Figure 4: Selected frames extracted from experiment video
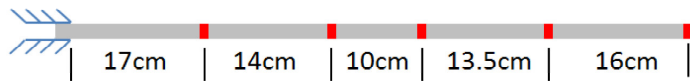
Figure 5: Distribution of tracked points along the hose

Figure 6: Trajectories of tracked points during the experiment over 16 sec
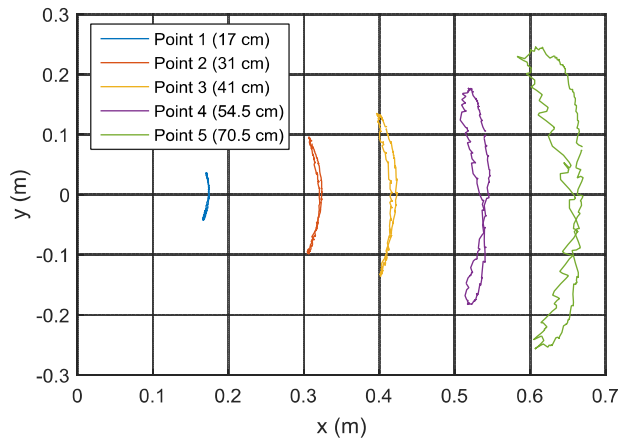
3.2 Simulation setup

The hose was modeled as 36 structural sections of 2cm each. The bending stiffness and damping coefficient were estimated by the method described in the appendix. The main parameter set to the fluid and structural solvers are presented in Table 1, Table 2 and Table 3.

Table 1: Fluid simulation main parameters

Water mass flow rate (g/s)	16.52
Air mass flow rate (g/s)	0.24
Outlet pressure (kPa)	101
Holdup for slug initiation (-)	0.43
Air buffer tank volume (cm^3)	600
hose Internal diameter (mm)	6
Roughness (mm)	1e-2

Table 2: Fluid solver spatial and temporal meshes

Minimum slug length (mm)	6
Minimum bubble length (mm)	10
Maximum bubble length (mm)	50

Table 3: Structural simulator main parameters

Mass per unit length (g/m)	44
Bending stiffness (N m^2)	3e-3
Axial stiffness (N)	500
Maximum time step (s)	1e-4
Element length (mm)	20
Kinetic friction coefficient (-)	0.3

Due to the limitations of the fluid dynamic model to reproduce surface tension effects on small diameter pipes, the slug initiation holdup (liquid volume fraction) was set to 0.43 in order to stimulate the slug generation. This configuration produced around 3 slugs per second. The liquid holdup time series at the outlet between 23 and 25 seconds is plotted on Figure 7.
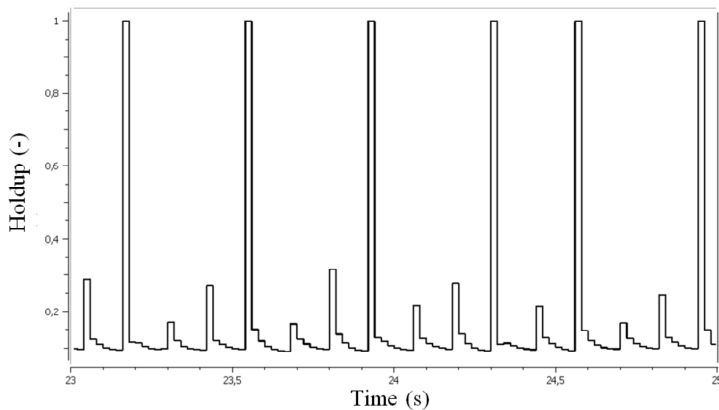
Figure 7: Simulated holdup time series at outlet

4 RESULTS AND DISCUSIONS

The simulation results reproduced the fluttering behavior observed on the experiment. Six representative pipe shapes during a same flutter cycle are shown in Figure 8. The trajectories of five points nearby the ones tracked in the experiment are presented on Figure 9. The maximum deflection from the straight configuration was over-predicted in 50%.

(a)

(b)

(c)

(d)

(e)

(f)

Figure 8: Selected frames extracted from simulation results. Dark blue areas represent liquid-filled volume

The period of fluttering was also compared and in this case, it was under-predicted by 30%. Figure 10 shows experimental and simulated time series corresponding to the farthest tracked point from the clamped point.
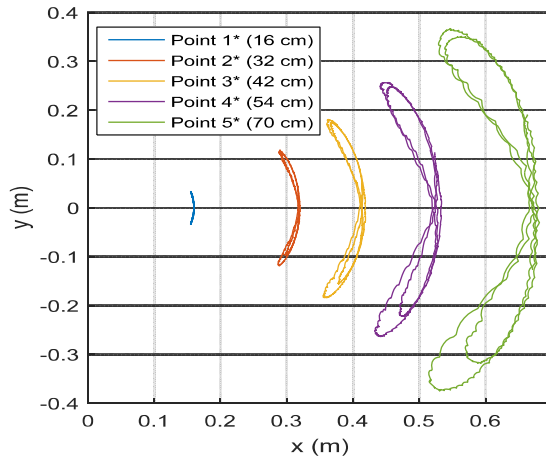
Figure 9: Trajectories of tracked points from the simulation over 20 sec
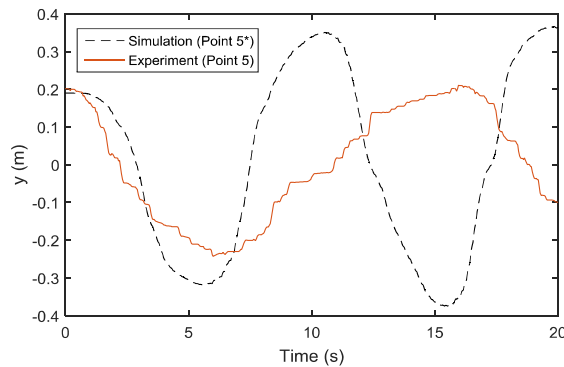
Figure 10: Traversal displacement of points 5 and 5* over 20 s

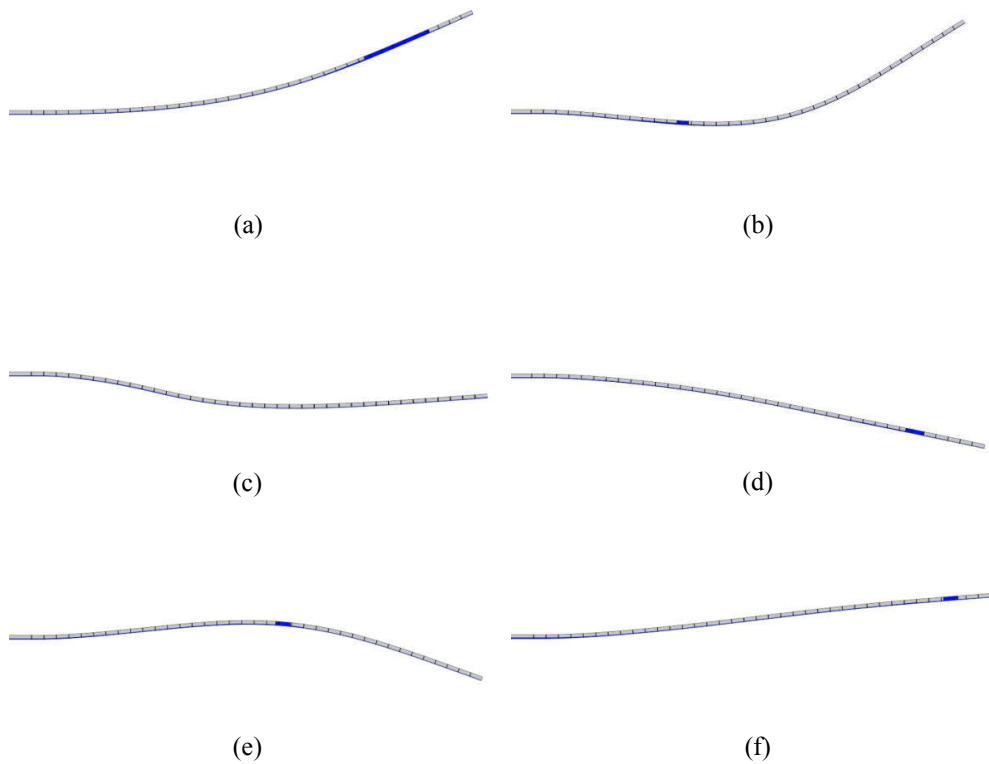The wider "8" shape described by the trajectory of almost all the tracked points indicate a larger hose curvature on the simulated results. This may indicate a wrong estimation of bending damping by neglecting the internal flow induced damping.

Although a quantitative analysis of the predicted displacement can be improved, the presented model demonstrates important details of the dynamics of the fluid-structure interaction.

It is worth to note that some of the parameters introduced in the simulation like friction coefficient and slug initiation holdup were estimated due to lack of information on the experiment conditions.

5   CONCLUSIONS

- Experiment and simulations of a fluid-structure interaction case were carried out on a horizontal cantilever pipe conveying air-water slug flow.

- The implemented fluid-structure interaction model reproduced qualitatively the physics of a flexible pipe conveying gas-liquid flow.
- Differences in amplitude and oscillation period may be a consequence of not including two-phase internal fluid induced damping. The results will also be dependent on slug initiation models for small diameter pipes, as well as the friction between pipe and surface.

ACKNOWLEDGMENT

REFERENCES

[1] F. B. Seyed and M. H. Patel, "Considerations in Design of Flexible Riser Systems," presented at the Proceedings of the Second (1992) International Offshore and Polar Engineering Conference, San Francisco, USA, 1992.

[2] A. Ortega, A. Rivera, O. J. Nydal, and C. M. Larsen, "On the Dynamic Response of Flexible Risers Caused by Internal Slug Flow," presented at the ASME 2012 31st International Conference on Ocean, Offshore and Arctic Engineering, Rio de Janeiro, Brazil, 2012. Paper number OMAE2012-83316

[3] A. Ortega, A. Rivera, and C. M. Larsen, "Flexible Riser Response Induced by Combined Slug Flow and Wave Loads," presented at the ASME 2013 32nd International Conference on Ocean, Offshore and Arctic Engineering, Nantes, France, 2013. Paper number OMAE2013-10891

[4] O. J. Nydal, "Dynamic Models in Multiphase Flow," *Energy & Fuels,* vol. 26, pp. 4117-4123, 2012.

[5] T. K. Kjeldby, "Lagrangian three-phase slug tracking methods," Ph.D. Doctoral thesis, Department of Energy and Process Engineering, Norwegian University of Science and Technology (NTNU), Trondheim, 2013.

[6] R. Ghadimi, "A Simple and Efficient Algorithm for the Static and Dynamic Analysis of Flexible Marine Risers," *Computers & Structures,* vol. 29, pp. 541-555, 1988.

[7] A. Gravelle, A. Ross, M. J. Pettigrew, and N. W. Mureithi, "Damping of tubes due to internal two-phase flow," *Journal of Fluids and Structures,* vol. 23, pp. 447-462, 2007.

[8] F. Vera, Rivera, R., Nuñez, C., "Backward Reaction Force on a Fire Hose, Myth or Reality?," *Fire Technology,* pp. 1-5, 2014.

[9] R. Clough, Penzien, J., *Dynamics of Structures*, Third ed.: Computers & Structures, Inc., 2003.

APPENDIX

The hose bending stiffness and damping coefficient were estimated as follows: the hose was installed as a vertically hanging cantilever. The free end was displaced and released to trigger pendulum oscillations. The previously mentioned video recording and processing technic was employed to track the free end of the hose during the experiment. Then the period of oscillation and logarithmic decrement of amplitude were calculated. The same experiment

was simulated in the structural dynamic software described on section 3.1. Different values of bending stiffness and damping coefficient were tested until obtaining results fairly close to the experiment. Figure 11 presents the amplitude per cycle measured from the experiment and the simulation results with a bending stiffness of 0.001 N m^2.
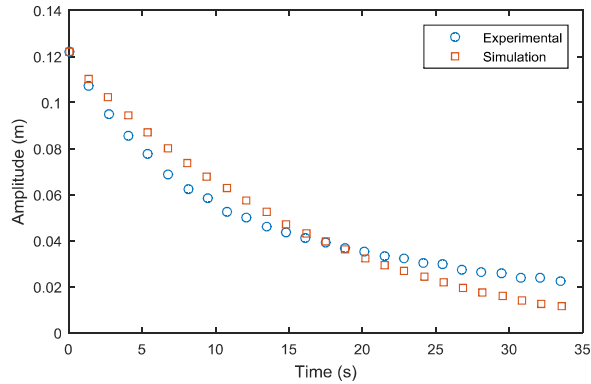

Figure 11: Calibration of bending stiffness. Measured and simulated amplitude of oscillation of a hanging pipe

Paper 2 - Two-Way Fluid-Structure Interaction in a Flexible Pipe Conveying Gas-Liquid Slug Flow

OTC-26167-MS

Two-Way Fluid-Structure Interaction in a Flexible Pipe Conveying Gas-Liquid Slug Flow

J. Vieiro, E. I. Ita, and O. J. Nydal, Norwegian University of Science & Technology

Abstract

Some cases of marine operations with pipes conveying multiphase flows can show structural movements depending on the internal flow dynamics. A floating pipe conveying two-phase gas-liquid flow is an example where a two-way coupling between the internal flow and the structural dynamics is needed. The objectives of the paper is to demonstrate a method for dynamic coupling of slug flow and pipe structure simulations by comparing numerical results with small scale experiments on flexible pipes.

Two small scale experimental setups for two-phase slug flow in floating and submerged flexible pipes were prepared. The experiments were designed to give unstable flows. The air and water flow rates were measured and the pipe movements were video recorded. A new coupled model was established, in which a structural dynamic model has been implemented into a dynamic slug tracking model. Forces due to the internal flow such as fluid weight, friction and centrifugal force were included in the structural model, as well as external fluid drag and soil contact forces among others.

The implemented model can reproduce fairly well the dynamic forces due to the internal flow as well as predict the associated pipe deformations and movements. Slug flow can potentially have an impact on pipe dynamics, in particular for cases where severe slugging can occur.

Introduction

The numerical analysis of flexible production risers conveying multiphase flow is commonly divided in two fields: dynamics of internal flow in order to predict pressure drops, flow patterns, transient effects, among others; and structural analysis to estimate the forces and deformations of the structure, as well as stresses and vibrations.

When an offshore flexible riser is exposed to severe slugging, the density of the internal fluid undergoes large variations as the riser can be filled with liquid which blows out at regular intervals. This change in the internal density, as well as the fluid-wall forces during the violent blowout, can have an important effect on the riser geometric configuration. At the same time, a change in geometry can have an important effect on the slugging phenomenon [1]. Since a dip in a pipe can accumulate liquid, the increased gravity force on the structure can increase the dip further.

In this paper we demonstrate a direct two-way coupling between a dynamic model of internal two-phase flow and a flexible pipe model. The influence of the internal gas-liquid flow on the geometry

of a flexible pipe and the effect of the pipe geometry on the flow is studied by including a structural dynamic model into a preexisting fluid dynamic framework. Floating and submerged pipes were chosen as test cases. Laboratory scale experiments and numerical simulations were carried out and the results were compared qualitatively and quantitatively.

Background

There are limited references concerning the influence of slug flow on the dynamics of flexible risers. One of the simplest models to take into account the internal slug flow on the response of offshore risers use a parametric description of the slugs as done by Patel and Seyed [2]. The density of the internal flow was modelled as a sinusoidal variation in time and a solution technique based on linearized frequency-domain dynamic analysis was applied. They showed that the effects of dynamic excitations due to momentum changes are important in the dynamic response of flexible risers because it can expose the riser to large tension fluctuations at the frequency of the plugs, and it can produce a dynamic change on the geometric stiffness of the riser due to effective tension variations.

Seyed and Patel [3] showed through a numerical example that forces induced by severe slugging can exceed very adverse environmental loads on lazy-S shaped risers.

Gundersen et al. [4] developed a methodology to determine the remnant fatigue life of flexible risers under vessel motion, continuous and regular slug flow and external irregular wave loading. This work was based on the use of two commercial simulators: one to perform a global analysis on a riser in order to find the response of the riser under given loads, and a local analysis to determine the stress transfer function and the stress time series of the tensile wires on the riser wall. In a case study, they showed that slug flow can reduce the riser fatigue life approximately by 50%.

Connaire et al. [5] studied the dynamic response and stress distribution in a compliant riser base spool by means of a subsea structures analysis software. They conclude that the exclusion of the load due to slugging can result in an important underestimation of the stress ranges on compliant subsea steel systems.

Some two-way coupled fluid-structure interaction (FSI) studies in offshore pipes have been carried out in recent years. Jia [6] performed coupled 3D computational fluid dynamic (CFD) and 3D computational structural dynamic (CSD) simulations in a pipeline span, jumpers and a riser using commercial software. The FSI procedure was implemented by user defined subroutines and build-in functions in both simulators. The slug formation and decay in vibrating pipes could be identified, and the vibration itself was generated by the same multiphase flow phenomenon.

Elyyan et al. [7] studied one-way and two-way FSI in an M-shaped jumper subject to oil-gas slug flow during start-up. They also used a commercial software package with build-in coupling CFD-CSD system. They showed that the one-way coupling underestimate the peak deformation by about 100%, compared with two-way simulation results. On the other hand the one-way coupling approach was sufficient to capture the maximum deformations and dominant frequencies at steady operation for the given conditions.

Ortega et al. [8] studied the influence of the slug flow on a lazy wave riser dynamics by exchanging information between two independent in-house computer programs. The coupling was made using the High Level Architecture standard to transfer the geometric configuration from the structural simulator to the fluid simulator, and to transfer the mass and velocity of each phase in the reverse direction, so the programs provide two-way dynamic feedback. A lazy wave riser with air-water slug flow was simulated and irregular loads in the structure due to the characteristics of the flow were obtained.

Ortega et al. [9] carried out a study similar to [8] but in this case using a non-lineal finite element formulation in the structural simulator. They simulated the dynamic response of a catenary riser under the effects of internal hydrodynamic slug flow and external regular waves. The results showed the influence of the external flow on the generation of hydrodynamic slugs because of the change in riser geometry, and the amplification of the dynamic response due to the interaction between the external and internal forces.

Using transparent flexible pipes in laboratory-scale experiments, some researchers have been able to study the internal pipe flow and at the same time, quantify the displacements of the pipe. Bordalo et al. [10] studied the influence of two phase gas-liquid internal flow on a flexible catenary riser through a series of experimental tests on a scaled riser system. The riser was surrounded by stagnant air. The gas and liquid flow were adjusted to reproduce slug, churn and annular flow patterns. They observed that the movement of the riser increases when increasing the gas flow rate from slug flow to churn-annular transition, and decreases on fully annular flow. They conclude that the internal flow plays a significant role on the structural dynamics of slender catenary risers.

Silva [11] studied the influence of externally induced top end oscillations in the air-water flow patterns and pressure drop in a vertical riser. The conclusion was that the flow patterns were almost unaltered by the top end motion, however the pressure drop increases when the oscillation frequency increases, for the flow patterns of bubble, slug or churn flow.

Evangelista and Bordalo [12] ran experimental tests to study the effect of the surrounding fluid on the dynamics of a catenary pipe conveying slug flow. They observe greater displacement amplitude when the pipe is surrounded by air than when it is submerged in water. They also reported lower oscillation frequency when the pipe is submerged in water.

Numerical model

The main features of the internal fluid flow simulator as well as the basic equations of the structural dynamic model will be presented in this section, followed by the coupling procedure of the two models.

Internal hydrodynamic model

The internal flow dynamics were solved using a one-dimensional two-fluid model based on slug capturing and slug tracking formulation [13]. The fluid regions (bubbles and slugs) are decribed by a dynamic mesh, and each of these regions can have a subgrid (sections) as shown in Figure 1.
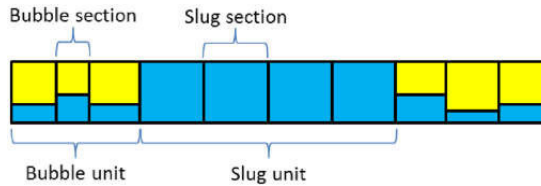
Figure 1—Mesh in the slug tracking scheme

The slug units are modeled as incompressible fluid and the gas units as compressible using the two-fluid model [13], so that mass, momentum and energy equations are solved for liquid and gas phases. Phase fractions are obtained from mass equations. Using a stationary fluid grid, liquid slug formation can be captured from the two-fluid model. After a slug is generated, the grid is updated in order to track the slugs and bubbles along the domain.

The mass conservation equation for a fluid phase K is stated by (no phase change):

$$\frac{\partial \alpha_k \rho_k}{\partial t} + \frac{\partial (\alpha_k \rho_k U_k)}{\partial l} = 0 \tag{Eq. 1}$$

where α is the volume fraction, ρ is the density, U is the average fluid velocity, is the time and t is the coordinate along the pipe.

The momentum equation for a phase K is given by:

$$\frac{\partial(\alpha_k \rho_k U_k)}{\partial t} + \frac{\partial\left(\alpha_k \rho_k U_k^2\right)}{\partial l} = -\alpha_k \frac{\partial p}{\partial l} - F_{wall,k} \pm F_{int,k} - G_k \tag{Eq. 2}$$

where p is the pressure field, $F_{wall,k}$ is the friction force between phase k and the pipe wall, $F_{int,k}$ is the interfacial friction force between phase k and another fluid phase, and G is the gravity force, including a term to take into account a level gradient force. More details can be found in [14].

Structural dynamic model

The pipeline is divided into elements with a node on each extreme. The node displacement $\vec{s}$, velocity $\vec{v}$, and acceleration $\vec{a}$ vectors relative to a stationary coordinate system are defined as follows:

$$\vec{s}_i = \begin{Bmatrix} x_i \\ y_i \\ z_i \end{Bmatrix} \qquad\qquad \vec{v}_i = \dot{\vec{s}}_i \qquad\qquad \vec{a}_i = \dot{\vec{v}}_i \tag{Eq. 3}$$

where subscript i represents a node as shown in Figure 2. Axial and bending stiffness and damping were reproduced by adding springs and dashpots between nodes (axial force) and around nodes (bending force). The mass of each element is lumped equally in its nodes.
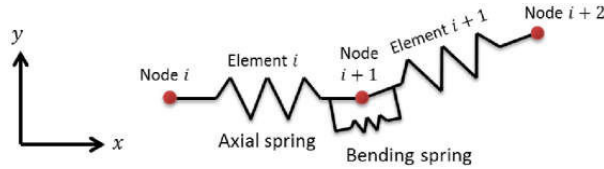

Figure 2—Schematic representation of the mechanical system

All the significant forces are calculated for each element and applied on its nodes. The dynamic equilibrium equation for each node is as follows:

$$\left(m_{s,i} + m_{F,i} + m_{V,i}\right)[I]\vec{a}_i = \vec{F}_i \tag{Eq. 4}$$

where $m_{s,i}$ is the structural mass, $m_{F,i}$ represents internal fluids mass (which are a result of the internal flow computation) and $m_{V,i}$ is the virtual mass.

The total force $\vec{F}$ over each node is the sum of the contribution of the internal (axial and bending), environmental (effective weigth, added mass force, drag, soil contact and floater mooring) and operational forces (internal flow weigth, centrifugal and wall friction forces):

$$\vec{F}_i = \vec{F}_{T,i} + \vec{F}_{B,i} + \vec{F}_{W,i} + \vec{F}_{V,i} + \vec{F}_{D,i} + \vec{F}_{S,i} + \vec{F}_{M,i} + \vec{F}_{F,i} \tag{Eq. 5}$$

Time integration of Eq. 4 was done by Newmark beta method [15]. The equations of the structural dynamics were implemented in the pre-existing dynamic multiphase flow simulator [16], so the resulting software is a stand-alone application.

Fluid–Structure coupling

The computation sequence was made as follows:

1. Initialize fluid and structural domains using initial conditions.
2. Solve the internal fluid equations.
3. Update fluid mesh if necessary.
4. Update mass, velocities and volume fraction of gas and liquid phases on each structural cell.
5. Calculate internal, environmental and operational forces.
6. Solve dynamic structural equations.
7. Update pipeline geometry according calculated displacements.

8. Move one time step forward and repeat the calculation from step 2 until final time is reached.

Experimental set-up and results

Two flexible hose experiments were selected as demonstration cases:

Case 1. Floating hose   The first experiment consisted of a 10 m long hose floating in a pool connected to an air-water feed system and a floater linked to ground by a spring as shown in Figure 3. An inlet buffer tank was included to generate severe slugging conditions. An underwater video camera was installed and the pipe movement was recorded on video files.
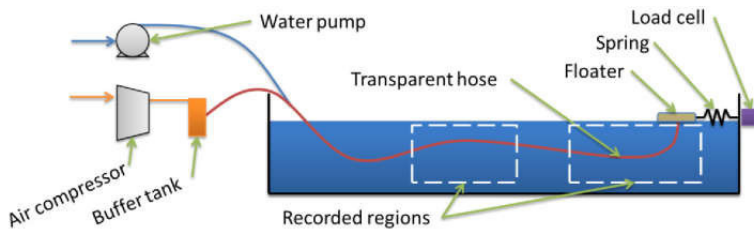

Figure 3—Sketch of the floating hose experimental set up

In the recorded video it was possible to observe how the pipe sinks to the button until a long bubble (about 50 diameters length) penetrate beyond the pipe-soil contact point. Due to the reduction of fluid weigth, the pipe slowly starts to rise. After this bubble is out of sight, a train of bubbles-slugs having different size (from 2 to 40 diameters long, Figure 4) flows at a higher speed. The consequential reduction in internal fluids weigth pushes up part of the pipe to the water surface and the flow velocity starts to reduce until no bubbles can be observed. The incoming liquid accumulates in the pipe dips making it sink again, iniciating a new severe slugging cycle. Four complete cycles were recorded, all of them looking alike to each other and having a period of about 45 seconds.

Figure 4—Image extracted from floating pipe experiment

Case 2. Catenary pipe   The second experiment consist of almost the same set up as the floating hose experiment, but some extra weights were attached to the pipe in order to reproduce a catenary-like shape. The displacement of the pipe and floater were recorded in video and the floater mooring force was logged using a load cell. The observed pipe displacements were much smaller in this case than in the floating hose experiment. Figure 5 shows a capture of the video recorded during gas blow out, and Figure 9 presents the mooring force on the floater. The severe slugging period was 61.3 seconds.

Figure 5—Image extracted from catenary pipe experiment

Numerical set-up and results

Both experiments were simulated using the model described above.

Case 1.Floating hose   The main parameters introduced to the models are shown in Table 1. The imposed structural boundary conditions (Figure 6) were:

- Displacements restricted to vertical plane (2D).
- The first two pipes of 2 meters long were completely fixed.
- Both ends of the flexible sections were always on the pool free surface. The last node was fixed in the vertical direction and restrained by a linear spring in the horizontal direction.
- The soil contact force was activated when the distance between the bottom and a node was less than the pipe external radius.

Table 1—Main parameters introduced to the simulator

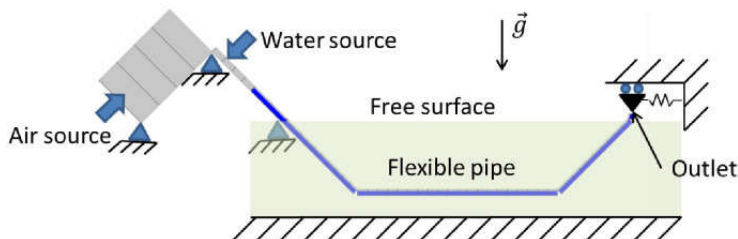|	
Flexible pipe length (m)	8
Element length (m)	0.2
Internal diameter (m)	0.012
External diameter (m)	0.016
Mass per unit length (kg/m)	0.118
Axial stiffness (N)	44
Bending stiffness ($N\,m^2$)	1.1
Buffer tank volume (m^3)	0.023
Water mass flow rate (kg/s)	4.1e-2
Air mass flow rate (kg/s)	5e-5
Spring stiffness (N/m)	1
Water density (kg/m^3)	1.0
Water level (m)	1.6

Figure 6—Imposed boundary conditions

The solver was run for 300 computational seconds. Figure 7 shows four pipe configurations during a severe slugging cycle. The sequence of events was as follows: As the upstream pressure increases, the tail of the slug moves downward to the outlet (Figure 7-a). The reduction of density in the upstream section increases the buoyancy force, so this section starts to rise (Figure 7-b). The slug is accelerating as it leaves the pipe. A second slug is generated in the upstream section before the first slug leaves completely the pipe (Figure 7-c). The second slug is accelerated and expelled from the pipe. The liquid amount in the pipe and the pressure in the buffer tank reach minimum values and the displacement of the floater achieves it maximum value. A third slug is generated (Figure 7-d) and the remaining liquid merges with it. The pipe sinks and the cycle initiates again (Figure 7-e).
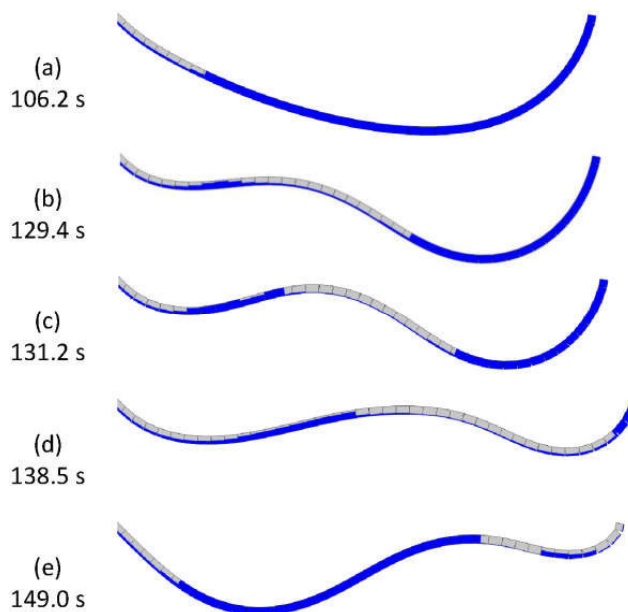

Figure 7—Simulation results for geometry and liquid fraction during a severe slugging cycle, floating hose case

A clear severe slug cycle of about 44 seconds was obtained from simulation, less than 3% smaller than the experimental period. The structural displacement cycle was fully linked with the internal fluid cycle. When the liquid inside the pipe is enough for the pipe to reach the pool bottom, the pipe velocity reduce almost to cero (Figure 7-a). This nearly static configuration gives the opportunity of synchronization to both cycles.

Case 2. Catenary pipe Extra masses of 0.28 *kg* were added to the floating hose at 2.5, 3.5, 4.5 and 6.5 m from the mixing section. The solver was run for 300 computational seconds. The gas and liquid flow rate were set to 5.6e-6 and 4.16e-2 *kg/s* respectively. The mooring spring stiffness was set to 10 *N/m*. The results reproduced severe slugging behavior as shown in Figure 8.
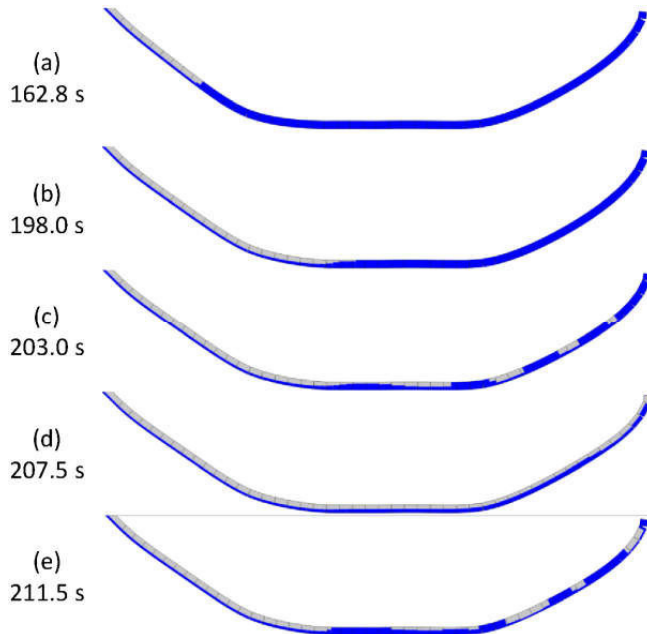
Figure 8—Simulation results for geometry and liquid fraction during a severe slugging cycle, catenary case

Figure 8-a shows the instant of maximum liquid accumulation. As the upstream pressure increases, the slug is pushed downstream. Air penetrates the lower point of the pipe (Figure 8-b). The pressurized air blows out the pipe (Figure 8-c and Figure 8-d). The water accumulates in the lower point and almost no fluids are produced (Figure 8-e). The period of severe slugging was 61.5 seconds, 0.3% larger than the experimental period. The variations in pipe geometry were smaller compared with the floating pipe experiment. Mooring force on the floater obtained from experiment and simulation are shown in Figure

Figure 9—Experimental and simulation results for mooring force on floater, catenary case

9.

Conclusion

A coupled two-way fluid-structure interaction simulator has been established by incorporating a structural model into a preexisting multiphase flow modeler. Some simulations were 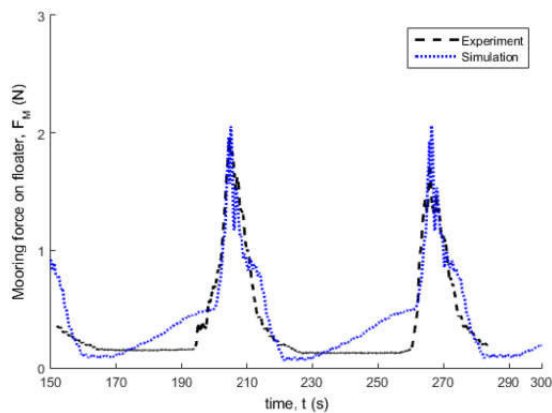carried out in order to reproduce experiments with a flexible pipe in a water pool conveying air-water two-phase flow. The coupled model was able to reproduce fairly well the pipe shape and internal flow behavior during severe slugging cycles, as observed from video recording in experimental tests.

Acknowledgments

Nomenclature

$\vec{a}$:	Node acceleration
$\vec{F}$	Force
G:	Gravity force
I:	Identity matrix
l:	Coordinate along the pipe
m:	Mass
p:	Pressure
$\vec{s}$:	Node displacement
t:	Time
U:	Average fluid velocity
$\vec{v}$:	Node velocity
α:	Volume fraction
ρ:	Density

Subindex

B:	Bending
D:	Drag
F:	Internal fluid
i:	Node number
int:	Interfacial friction force between fluid phases
k:	Fluid phase
M:	Mooring
s:	Structural, including pipe wall and attached mass
S:	Pipe-soil interaction
T:	Tension
V:	Virtual mass
W:	Weigth
$wall$:	Friction force between phase a fluid phase and the pipe wall

References

1. A. Moros and P. Fairhurst, "Production riser design: Integrated approach to flow, mechanical issues," *Offshore,* vol. **59,** 1999.

2. M. H. Patel and F. B. Seyed, "Internal Flow-Induced Behavior of Flexible Risers," *Engineering Structures,* vol. **11,** pp. 266–280, Oct 1989.

3. F. B. Seyed and M. H. Patel, "Considerations in Design of Flexible Riser Systems," presented at the Proceedings of the Second (1992) International Offshore and Polar Engineering Conference, San Francisco, USA, 1992.

4. P. Gundersen, K. Doynov, T. Andersen, and R. Haakonsen, "Methodology for Determining Remnant Fatigue Life of Flexible Risers Subjected to Slugging and Irregular Waves," presented at the ASME 2012 31st International Conference on Ocean, Offshore and Arctic Engineering, Rio de Janeiro, Brazil, 2012.

5. A. Connaire, J. Payne, J. McLoughlin, A. Connolly, and W. K. Kavanagh, "Slug Response in Subsea Piping: Advancements in Analytical Methods," presented at the Offshore Technology Conference, Houston, Texas, USA, 2013.

6. D. Jia, "Slug Flow Induced Vibration in a Pipeline Span, a Jumper and a Riser Section," presented at the Offshore Technology Conference, Houston, Texas, USA, 2012.

7. M. A. Elyyan, Y. Y. Perng, and M. Doan, "Fluid-Structure Interaction Modeling of a Subsea Jumper Pipe," presented at the ASME 2014 33rd International Conference on Ocean, Offshore and Arctic Engineering, San Francisco, California, USA, 2014.

8. A. Ortega, A. Rivera, O. J. Nydal, and C. M. Larsen, "On the Dynamic Response of Flexible Risers Caused by Internal Slug Flow," presented at the ASME 2012 31st International Conference on Ocean, Offshore and Arctic Engineering, Rio de Janeiro, Brazil, 2012.

9. A. Ortega, A. Rivera, and C. M. Larsen, "Flexible Riser Response Induced by Combined Slug Flow and Wave Loads," presented at the ASME 2013 32nd International Conference on Ocean, Offshore and Arctic Engineering, Nantes, France, 2013.

10. S. N. Bordalo, C. K. Morooka, C. C. P. Cavalcante, C. G. C. Matt, and R. Franciss, "Whipping Phenomenon Caused by the Internal Flow Momentum on the Catenary Risers of Offshore Petroleum Fields," presented at the ASME 2008 27th International Conference on Offshore Mechanics and Arctic Engineering, Estoril, Portugal, 2008.

11. E. S. Silva, "Estudo do escoamento bifasico em risers em movimento na produção maritima de petroleo em aguas profundas," *Master Thesis, Faculdade de Engenharia Mecânica,* Universidade Estadual de Campinas, Campinas, SP, Brazil, 2006.

12. Z. S. Evangelista and S. N. Bordalo, "Experimental set up to study the oscillation induced by two-phase flow in small scale models of production risers for offshore petroleum fields," presented at the 22nd International Congress of Mechanical Engineering (COBEM 2013), Ribeirão Preto, SP, Brazil, 2013.

13. O. J. Nydal, "Dynamic Models in Multiphase Flow," *Energy & Fuels,* vol. **26,** pp. 4117–4123, 2012.

14. T. K. Kjeldby, "Lagrangian three-phase slug tracking methods," Ph.D. Doctoral thesis, *Department of Energy and Process Engineering,* Norwegian University of Science and Technology (NTNU), Trondheim, 2013.

15. R. Clough, Penzien, J., *Dynamics of Structures,* Third ed.: Computers & Structures, Inc., 2003.

16. T. K. Kjeldby and O. J. Nydal, "A Lagrangian three-phase slug tracking framework," *International Journal of Multiphase Flow,* vol. **56,** pp. 184–194, 2013.

Paper 3 - Experimental and Numerical Simulation of Coupled Two-Phase Flow and Structural Dynamic of a Collapsed Flexible Pipe on the Seabed

EXPERIMENTAL AND NUMERICAL SIMULATION OF COUPLED TWO-PHASE FLOW AND STRUCTURAL DYNAMIC OF A COLLAPSED FLEXIBLE PIPE ON THE SEABED

J. Vieiro, A. K. Hemeda & O. J. Nydal, *Norwegian University of Science and Technology, Norway*

ABSTRACT

A computational scheme for coupled simulations of internal multiphase flow and structural dynamic is presented. The coupled model consists of a 1D two-phase flow simulator and a 3D structural dynamic simulator based on lumped mass formulation. The flow simulator features slug capturing and tracking functions in which a stationary grid is applied until a slug is created, then the grid is dynamically updated in order to track the slugs. The moving grid is interfaced with a fixed grid for the structural dynamic model. Axial and bending forces are calculated including internal fluids weight, friction and centrifugal force, and other forces like pipe-soil contact and external drag.

The scheme is demonstrated on a two-way coupling case: a submerged flexible pipe that has both ends fixed and its middle section is free to buoy and sink depending on the internal flow density.

In order to validate the coupled solver, small scale experiments were carried out. The experimental setup consisted of a 1.7 m long and 1.5 cm internal diameter transparent silicon hose submerged in water. A mixture of air and water was pumped into the system. The displacement of the hose and the internal flow pattern were recorded by a digital video camera. From video processing it was obtained fairly good agreement on slugs and pipe displacement frequencies between experiments and simulations.

The case relates to a phenomenon observed from ROV (Remotely Operated Vehicle) video recordings during the Macondo oil spill (Gulf of Mexico, 2010). From some of the mentioned videos, it can be observed a periodic motion of a section of the riser as well as periodic oil or gas dominated flow at the riser outlet. Some simulations of this case were run based loosely on data made public after the oil spill quantification research. Features observed on the ROV recordings were numerically reproduced. Results are discussed and compared with an expert report presented during the oil spill trial.

1.   INTRODUCTION

Gas-liquid flow in flexible pipes may have an important effect on the structural configuration and on the resulting flow pattern [1]. When the effective weight of a flexible pipe oscillates between positive and negative values, vertical displacements of pipe sections may cause accumulation of the heavier phase in dips. This accumulation may lead to unstable flow patterns.

This work is a continuation of [2] and [1] where fluid-elastic instabilities and a floating pipe conveying air-water flow were simulated and compared with small scale experiments.

An interesting case of two-way Fluid-Structure Interaction (FSI) was present during the Macondo oil spill. ROV video recordings showed a periodic displacement of a section of the riser, and evidence of slug flow was observed at the riser

outlet [3]. These two features had the same period. During the oil spill trial, these features were taken into account in an attempt to quantify the flow rate as presented in an expert report [3]. In the analysis done by [3], different flow rates were tested on a moving domain (the structural displacements following ROV video recordings) in order to reproduce the liquid holdup observed on ROV video recordings. [3] concluded that the alternating gas and liquid dominated flows observed at the riser end were caused by the riser motion.

The present study aim to show a method in which the structural displacement is considered a variable and is solved together with the internal fluid flow. Two cases of study are presented: a small scale experiment consisting of a submerged bend hose and a large scale case loosely based on data extracted from [3].

2.   DYNAMIC MULTIPHASE FLOW MODEL

A 1D hybrid slug capturing and tracking scheme was employed as dynamic multiphase solver for internal flow. The fluid domain is discretized in bubble and slug sections as shown if Figure 1. Mass, momentum and energy conservation equations are solved on each section. The domain discretization remains constant when there are not slug sections. If there are slugs present, the mesh is updated following the displacement of each one of them. Liquid phase was modelled as incompressible and the gas phase as real gas.
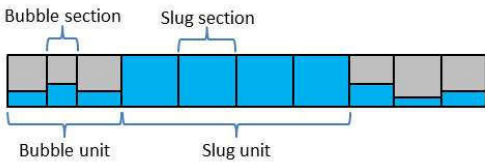

Figure 1. Basic discretization of fluid domain.

3.   DYNAMIC STRUCTURAL MODEL

The lumped mass model was selected due to its simplicity and ease of implementation. In this model, the pipeline is divided in straight sections, each of them having one node at each end. The sections are connected to their neighbours by the nodes, where the mass of each structural section is lumped. The sections are then modelled as massless springs and dampers as shown for three elements in Figure 2. In order to include internal shear forces, bending springs and dampers (not shown in Figure 2) were included in the model. Forces due to torsion were not included.
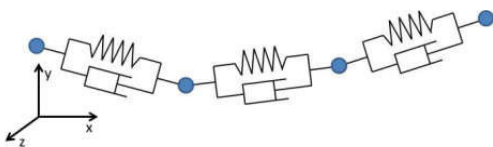

Figure 2. Modelling of the pipe structure (bending springs and dampers not shown here)

Some forces due to the surroundings were included: pipe-floor contact, buoyancy, drag on stagnant fluid and virtual mass force.

4.   DYNAMIC FLUID-STRUCTURE COUPLING

The coupling variables selected for this work were:
• Mass, velocity, volume fraction and wetted perimeter for each internal fluid phase.
• Structural elements inclination.

Internal flow variables were used in order to calculate internal flow induced forces on the structure. On the other hand, pipe inclination may have an important impact on flow pattern [4, 5].

5.   EXPERIMENTAL SETUP

In order to validate the described computational scheme, a small scale flow loop was designed and built. A sketch of the experimental setup is shown in Figure 3. The air supply line consists of a reciprocate compressor and a buffer tank of 625 cm3. A centrifugal pump drives water from a storage tank to the test section. Air and water supply lines are combined just before entering the hose. The hose layout is sketched on Figure 3. The hose is partially submerged in a water tank. Two points of the hose were fixed to the water tank bottom in order to keep it on an "U" shape in the test section. The air-water mixture is then discharged to a sink at atmospheric pressure through the tank bottom. Two red labels were attached to the "U" section of the hose (Figure 4) in order to track them using the video processing technique described in the next section
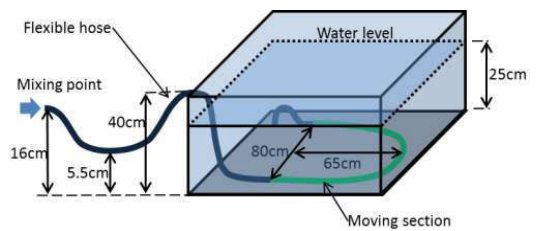

Figure 3. Sketch of experimental setup

A video camera was installed inside the water tank in order to record the displacement of the hose during the experiments.

The flexible pipe properties are presented in Table 1.

Table 1. Flexible pipe properties

Total length of the pipe (m)	3.2
Length of the moving section (m)	1.60
External diameter (cm)	2.20
Internal diameter (cm)	1.55
Bending stiffness (N m^2)	0.04
Axial stiffness (N)	880
Mass per unit length (kg/m)	0.23

Three different air-water flow rates were tested, all of them in the severe slugging flow pattern. The gas and liquid superficial velocities for all three cases are shown in Table 2.

Table 2. Gas and liquid superficial velocities for all studied cases

Case	Gas superficial velocity v_{sg} (m/s)	Liquid superficial velocity v_{sl} (m/s)
1	6.46e-2	6.15e-2
2	1.29e-1	6.15e-2
3	1.29e-1	1.53e-1

5.1   VIDEO PROCESSING

In order to extract the vertical displacement of the pipe, a MATLAB® script was developed. The video is separated in individual frames and each frame was decomposed in red, green and blue components. The red layer was subtracted from a grayscale representation of the frame in order to obtain the pixels occupied by each red label. The pixel coordinates are then converted to meters based on water surface and tank bottom locations. Figure 4(a) and (b) shows the maximum and minimum vertical position reached when the pipe is floating and completely resting on the bottom.

(a)

(b)

Figure 4. Video frames extracted from experiment Case 1 at: (a) maximum and (b) minimum hose vertical positions.

6.   NUMERICAL SETUP

The numerical domain was constructed based mainly on the experimental parameters presented in Table 1. The Structural domain is shown on Figure 5. It consists of a large diameter pipe reproducing the gas buffer tank and a sequence of pipes of the same diameter describing the experimental geometry. The structural domain was divided in 53 elements, 19 of them completely fixed and 34 elements free to move. All of moving elements had the same length of 5.0 cm.

On the other hand, the fluid domain was discretized using section lengths from 1.6 cm to 5.0 cm. The gas source was set inside the buffer tank and the liquid source just downstream of the buffer tank. The outlet pressure was set to atmospheric condition. The working fluids were: air as ideal gas and water.
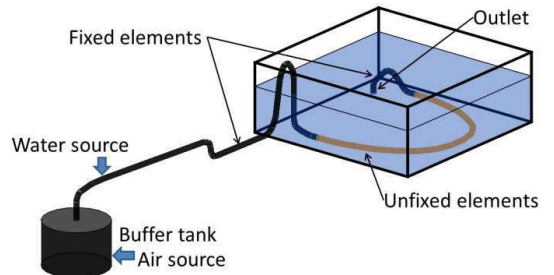

Figure 5. Sketch of structural domain at initial condition.

7. RESULTS AND DISCUSSION

The pipe elevation profile for seven instants of a same cycle from Case 1 are presented in Figure 6. It can be observed the slug generation and growing in the fixed section upstream the water tank (Figure 6a) until it reaches the highest point at l=2.4 m, followed by growing of a second slug in the first sag of the moving section (Figure 6b). As soon as the second slug reaches the middle point of the moving section, it begins to sink (Figure 6c). The moving section is pushed downwards due to the weight of the second slug, reducing the energy required to push the slug through the system (Figure 6d). After the blowout, most of the liquid is expelled from the system (Figure 6e). The remaining liquid is mainly accumulated on the dip formed between the moving section and the outlet peak and a new slug is rapidly formed on the fixed section outside the water tank.

(a) t=21.7 s

(b) t=33.7 s

(c) t=46.7 s

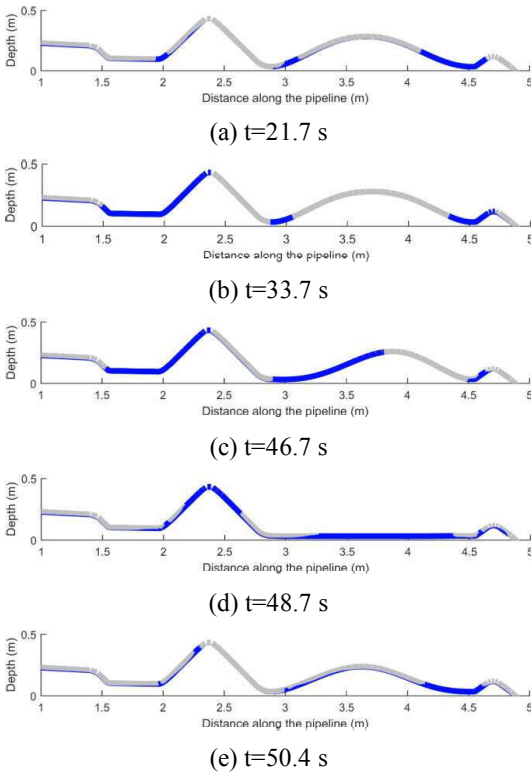
(d) t=48.7 s

(e) t=50.4 s

Figure 6. Snapshots showing simulation results for structural configuration and liquid holdup on Case 1. Blue area represents liquid volume fraction (Diameter is showed three times larger).

The vertical displacement of midpoint of the moving section is plotted as a function of time for the three cases (Figure 7, Figure 8 and Figure 9).
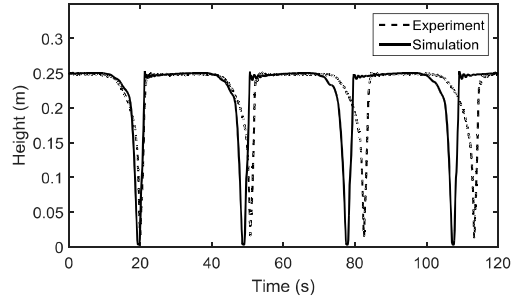

Figure 7. Measured and predicted vertical displacement during case 1.
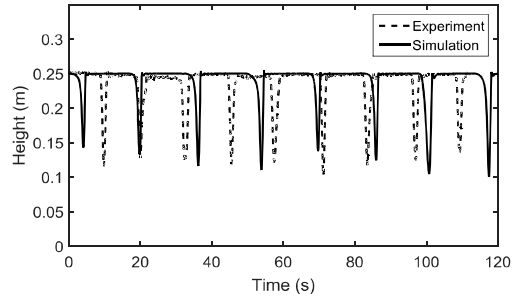

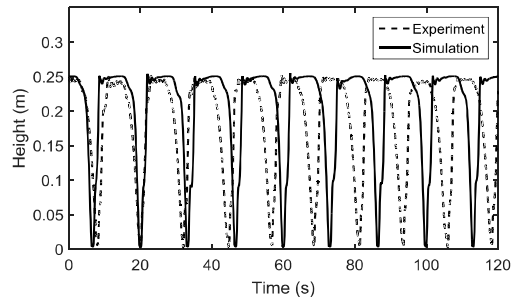Figure 8. Measured and predicted vertical displacement during case 2.

Figure 9. Measured and predicted vertical displacement during case 3.

It can be observed that the predicted slug-stroke period was lower than the experimental value for case 1. On the other hand, the period was over predicted for cases 2 and 3. Table 3 presents measured and predicted periods.

Table 3. Average slug-stroke period for experiments and numerical simulations

Case	Experiment	Simulation	Difference
1	33.1 s	31.1 s	-5.9 %
2	12.4 s	16.2 s	30.1 %
3	12.3 s	13.3 s	6.8 %

8. DEEPWATER HORIZON SLUG FLOW

The riser layout after the accident was extracted from plots presented on [3]. The domains were constructed from downstream of the kink at l=0, to the riser end at l=1327 m as shown in Figure 10, where l is the distance along the riser.
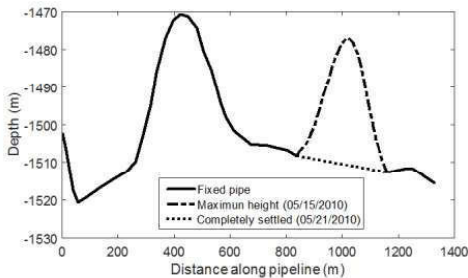

Figure 10. Riser profile when it is completely settled on the sea floor and at maximum height on 05/15/2010 (adapted from [3])

It is important to mention that this research was not intended to bring a new estimation of the amount of spilled oil, but to show a method for coupled analysis of fluid-structure interaction.

Significant differences were introduced, including: air-water flow instead of gas-oil, isothermal flow, no phase change, no kink, among others. The input parameters are presented on Table 4 and Table 5.

Table 4. Structural parameters of moving section

Length (m)	325
Number of elements (-)	30
External diameter (m)	1.20
Internal diameter (m)	0.355
Bending stiffness (N m^2)	8.0e7
Axial stiffness (N)	3.4e9
Mass per unit length (kg/m)	1100

Table 5. Input parameters for fluid simulation

Water mass flow (kg/s)	60.85
Air mass flow (kg/s)	14.60
Outlet pressure (Pa)	15e6
Temperature (K)	378

8.1 FIXED STRUCTURAL DOMAIN

A first simulation using a fixed geometry was run (Maximum height on Figure 10). A time independent stratified flow along the whole riser length was obtained for this case. The liquid holdup along the domain is plotted on Figure 11.
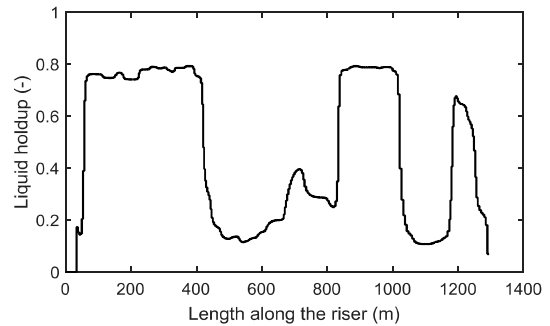
Figure 11. Liquid holdup along the riser for fixed geometry simulation

8.2 FIXED STRUCTURAL DOMAIN

For the second simulation, the profile given as initial condition was the profile after the riser was completely settled on the sea floor as shown on Figure 10. The displacements of nodes from l=835 m to l=1161 m were solved. The riser profile and liquid holdup are shown for four different instant in Figure 12.

It can be observed that results from l=0 to l=800 m do not differ significantly from the fully fixed riser simulation.

(a) t=1645s

(b) t=1721 s

(c) t=1780 s

(d) t=1813 s

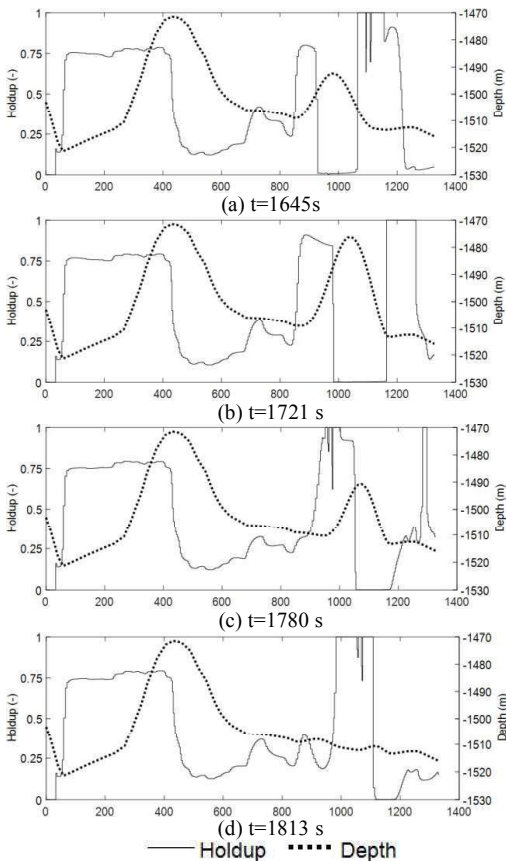—— Holdup ▪▪▪▪ Depth

Figure 12. Holdup and depth along the riser

Figure 12(a) presents a profile when the moving section is displacing upward. The liquid is accumulated on the upstream side of the moving section hill. The height of the moving section reach its maximum value (Figure 12(b)) and starts to sink due to the increasing mass of liquid (Figure 12(c)). The riser sinks to the bottom and the thick layer of liquid is now moving downhill due to seabed inclination (Figure 12(d)). As the liquid batch leaves the moving section, the pipe starts to rise again (Figure 12(a)). Liquid slugs were obtained downstream of the moving section. For this case, the period of riser movement was 240 s

The downward inclined section of 80 m at the end of the riser promotes stratified flow, so no liquid slugs were present at the riser end.

As found by [3], liquid and gas dominant flows were obtained at the riser end, having the same

period of the riser displacement. These features were not present in the fixed geometry simulation results, but are reproduced for the coupled solver case.

9.   CONCLUSIONS

Two-phase flow, two-way coupled fluid-structure interaction was experimentally and numerically studied in submerged pipes involving curved buoyant sections. Numerical results predicted quite well some features observed during the small scale experiments and large scale qualitative data.

In a large scale simulation, liquid batches were generated due to the movement of a pipeline section. Those batches contributed to create liquid slugs downstream, where fixed structure simulations predicted stratified flow.

REFERENCES
1.   J. VIEIRO, E. I. ITA & O. J. NYDAL, 2015 'Two-Way Fluid-Structure Interaction in a Flexible Pipe Conveying Gas-Liquid Slug Flow', OTC Brasil 2015,
2.   J. VIEIRO, A. K. HEMEDA & O. J. NYDAL, 2015 'Multiphase Flow in Flexible Pipes: Coupled Dynamic Simulations and Small Scale Experiments on Garden Hose Instability', Eighth National Conference on Computational Mechanics MekIT'15, 373-382.
3.   M. ZALDIVAR, 2013 'Quantification of Flow rate during slug flow', In Re: Oil Spill by the Oil Rig "Deepwater Horizon" in the Gulf of Mexico, on April 20, 2010. Available: http://www.mdl2179trialdocs.com/releases/release201310161045010/TREX-011683.pdf
4.   D. BARNEA, O. SHOHAM & Y. TAITEL, 1982 'Flow pattern transition for downward inclined two phase flow; horizontal to vertical', Chemical Engineering Science, 37, 5, 735-740.
5.   D. BARNEA, O. SHOHAM, Y. TAITEL & A. E. DUKLER, 1985 'Gas-liquid flow in inclined tubes: Flow pattern transitions for upward flow', Chemical Engineering Science, 40, 1, 131-136.

Paper 4 - Experimental and numerical study of a flexible floating pipe conveying multiphase flow

Paper 5 – Two way coupled fluid-structure interaction of a flexible riser conveying slug flow

Paper 6 - Multiphase flow in flexible pipes: simulations and small scale experiments

Multiphase flow in flexible pipes: simulations and small scale experiments

J Vieiro[a], Z Wang[b] and O J Nydal[a]

[1] Norwegian university of Science and Technology, Norway

[2] Southwest Petroleum University, China

ABSTRACT

Gas liquid slug flow can induce vibrations in process piping and large scale slugging can cause some oscillations of subsea flexible pipes. Pipe movements should be avoided, as fatigue can lead to pipe failure. Flow transients can also cause pipe failure, water slugs have lifted geothermal pipelines off support, and runaway hydrate plugs have caused fatalities. The flow - structure interaction is therefore of interest to study and to incorporate in dynamic simulators.

Several cases of dynamic slug flow-structure interactions have been studied in small scale laboratory. A two way coupling has been established between a pipe structure model and a slug tracking model.

A pigging case of a submerged flexible pipe is presented here. An initially liquid filled hose is hanging freely in a 4m long water tank. A pig is inserted at the inlet, and subject to a backpressure of air which drives the pig and the liquid out of the pipe. The subsequent pipe dynamics is video recorded and compared with the coupled flow-structure simulations. At high flow rates the initially U-shaped pipe rises above the water level and falls back to the surface. The experiments and the coupled models are described as well as key aspects of the numerical solvers.

INTRODUCTION

Flexible pipes are used to connect subsea pipelines to floating structures. As the floaters can have some movements with waves and wind, the connected pipe needs to have some flexibility. In order to reduce the top side structural forces, some buoyancy elements can be attached along the line. This can also contribute to pipe movements induced by sea currents, and also modify the structural response to the top side movements. Riser dynamics due to external forces has been a particular issue in ocean structural analysis, and several computer programs are available for dynamic simulations [1].

With the case of gas-liquid flows in the pipeline-riser system, the internal hydrodynamic forces on the pipe can also be time varying. For the case of severe slugging, with a regular filling and blow out of the riser, the forces can become large and influence on the riser structural dynamics. Some studies on severe slugging in fixed lazy wave shaped risers are reported in [2-6]. A coupling between a structural simulator and the current slug tracking model has also been tested in [7, 8].

The severe slug flow phenomenon is on large time and length scales, where the forces due to the change in the gravity of the two-phase flow mixtures are important. For shorter flow systems, normal hydrodynamic slug flow can excite high frequent structural vibrations. The main hydrodynamic force is now the changes in the velocity directions of slugs passing through pipe bends (centrifugal forces).

Some of the dynamic interaction of multiphase flow and flexible pipes require a two way coupling. These are cases where the internal two phase flow modifies the structure and the structure in turn modifies the internal flow. Examples which have been studied by simulations and by small scale experiments are the dynamics of a flexible riser collapsed on the sea bed [9] and a floating pipe [10]. A one way coupling

could be sufficient for other cases which have been studied likewise. In a garden hose instability [11], the internal slug flow induces a fan-like movement of a pipe laying on the a horizontal surface. The pipe movement may then not influence the high frequent slug flow in the pipe. In severe slugging in a lazy wave shaped riser, the large scale slugging induces pipe movements, but the movements are expected not to modify the slug flow characteristics, except possibly for flow conditions close to the stability limit.

Pigging is a particular type of flow transient, where a device is inserted into the pipe to clear out the pipe content (liquid or pipe deposits), or to inspect the pipe integrity. A pigging event gives a single transient force on the pipe as it moves from the injection point to the pipe outlet. Another similar type of single transient can be the accidental release of a hydrate plug under a high differential pressure. Such runaway plugs can be a safety threat for pipeline operators.

The case of pigging is demonstrated here. A small scale experiment is made with a pig clearing out the liquid of a submerged, hanging pipe. The experimental cases are described and the results compared with coupled flow-structure simulations.

NUMERICAL MODEL

Dynamic flow model

The natural procedure when designing a 1D dynamic multiphase flow model is to formulate the mass and momentum equations for both phases, discretize the equations with a suitable numerical method and solve the set of equations by implementation in a computer program. This set of quite general equations is then applied to the full range the different dynamic two phase flow cases which can occur in a pipeline. The propagation of gas-liquid fronts is then treated as a numerical challenge, where the main objective is to have the numerical method reproduce the mathematical solution of the set of equations.

As a pig is a new element in the flow case, and not just a result of the general set of equations, some sort of pig model and pig tracking is needed. This is possible to implement in a general framework, but it is not straight forward to make a projection scheme where a pig model modifies the fluxes on the general set of equations in such a way that it moves continuously across grid points.

The pig model applied here is implemented in a particular slug tracking scheme. The scheme is described and tested for different cases [12-14]. Here the model is summarized with focus on the principles for the case of pigging.

The starting point for the slug tracking model is the fact that the flow phenomenon has compressible elements (slug bubbles with separated flows) and incompressible elements (slugs, with possible gas entrainment). The model is then designed for this structure: separate flow models for the incompressible and for the compressible parts of the domain. The domains (slugs and bubbles) are tracked and exchange mass and momentum.

The basic features of the scheme have been described in [14]. Here the scheme is presented through a description of the object oriented data structure and the models for each structure.

Pipeline

The pipeline class holds the geometry of the pipeline, in terms of a linked list of pipes, each having individual inclinations. The computational grid for the gas and the liquid moves and gets the pipe properties from the pipeline class in each time step. The pipeline is also the grid for a dynamic structural model.

Units

Slugs and a bubble are "units", which are inherited from a unit base class. A unit has links to a sub grid and holds moving borders at each end. Units can be created or removed dynamically, as a result of the underlying mass and momentum balances solved in the sub grid.

Sections

Each unit manages its own grid, where the flow variables are solved. The sub grid is named "sections", and sections have linked borders between them. The sections hold pressure, phase fractions and temperatures, as well as classes for the conservation laws. The main types of inherited sections are bubble sections in bubble units and slug sections in a slug unit. "Borders" hold the velocities, so the combination of sections and borders give the data structure for the staggered grid solver.

Borders

Several border classes exist, all inherited from a parent border class. The borders have pointers to a pipeline class, in order to retrieve the pipe inclination as the borders move along the pipe. The main border classes are those for liquid-liquid, gas-gas and gas-liquid.

- A liquid-liquid border is between liquid sections, and typically provides phase velocities from a slip relation and a mixture velocity in the slug unit.
- A gas-gas border is between gas sections, and typically provides the gas and liquid velocities from two momentum equations, solved on a staggered grid between the neighboring sections.
- A gas-liquid border is either a bubble nose or a breaking front. A nose propagates in relation to the liquid velocity in the slug ahead of it, according to commonly used bubble nose propagation relations. A breaking front propagates according to the mass balances across the fronts. Selection criteria are needed to determine whether a front should be a nose or a breaking front.

Bubble unit

A general bubble unit solves the two fluid models on the sub grid in the bubble: a set of mass and momentum and energy equations for each phase. If a whole pipeline is a single bubble unit, the model is essentially equal to a standard two fluid model. With an averaged slug flow model implemented in the sections ("unit cell model"), together with stratified-slug flow transition criteria, then the 2 phase scheme becomes similar to the schemes which are implemented in the commercial models.

In a simplified version of the bubble unit, the pressure is approximated to be uniform along the bubble (quasi steady gas flow). This is most often a good approximation for normal slug flow, but not so for simulation of rapid plug transients.

Slug unit

An integral momentum equation is employed across a slug unit, giving a uniform mixture velocity along the incompressible slug.

Figure 1 shows units, sections, and borders in an example domain. The meaning of the variables are: P pressure, U_l liquid velocity, U_g gas velocity, U_m mixture velocity, H holdup (liquid volume fraction),
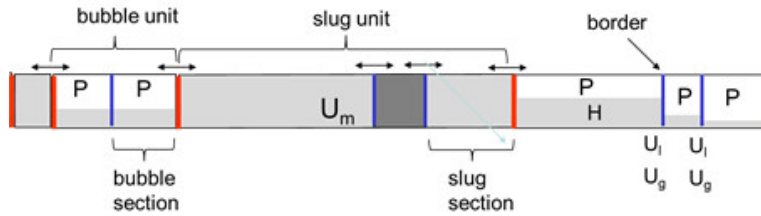
Figure 1. Data structure for flow model. The numerical grid is the sections (pressure, phase fractions) and borders (velocities). A pig is a slug section under the slug unit. A two fluid model is solved for the bubble unit grid. An integral momentum equation is solved for the incompressible slug unit. A subgrid in the slug unit gives the oil-water fractions due to a slip relation (not included in the figure).

Slug initiation

Slug initiation is the difficult part of the slug tracking model. Self-initiation from a two fluid model in the bubble unit is numerically possible, but difficult to get physically correct. The transition to slug flow is usually through a stage with wavy flow. The numerical slug initiation is also sensitive to the underlying numerical scheme.

Using a subgrid slug initiation model (e.g. similar as for flow regime transition criterion), within a large computational grid, gives computationally efficiency, as a small grid is now not necessary for capturing the initiation. It is, however, difficult to avoid grid dependencies when using subgrid slug initiation models.

Solver

A solver with implicit time integration is implemented outside the unit and section classes. The solver traverses the section lists and collects contributions to the coefficient matrix for two momentum equations, in which the pressure terms have been eliminated with a pressure equation (a volumetric flow balance with densities represented as pressure through a state equation). After solving for the velocities, the pressures are updated, and the mass equations give the fractions. The energy equations are optionally solved as the last task in each time step, before the grid management is made.

Grid management

The grid management is the task which takes the major effort when implementing a moving grid scheme.

The numerical grid for the flow model is structured in terms of units, sections and borders, and organized in linked lists. The reason for this structure is that it facilitates creation and removal of grid elements, and it facilitates the implementation of new elements, as exemplified with a pig in the current case.

Pig

A pig is implemented as a liquid section, and with associated pig-liquid and pig-gas borders. The friction and leakage properties are characteristics which are implemented in the pig class and border classes. After initiation of a pig (or several pigs) no further "if" tests should be needed in the flow model. Implementation of hydrate plug model can in principle be made similarly, in the form of a new liquid section and associated new hydrate borders. A melting model can then be developed and tested as a section class and the associated hydrate border (energy balances, gas release, friction etc.). The behavior in the flow model should then follow without the need for further modifications in the flow model.

DYNAMIC STRUCTURE MODEL

A lumped mass model for structural dynamics is included in the framework. A node class is created, containing the mass of the pipe wall, internal fluid and added mass from the surroundings, as well as all the applied forces (internal, environmental and flow induced forces). The wall axial force is modeled as linear springs and dampers along the pipes, while the bending force is modeled as angular springs and dampers around nodes.

As a pipe might contain many different sections at different time instants, an algorithm for mapping variables from the fluid grid into the fixed structural grid is required. Variables such as mass, velocity and density of each phase are mapped on the pipe objects. Based on these variables, forces due to internal flow are calculated and applied on the nodes of each pipe. The external hydrodynamic forces are modelled using the Morrison equation as presented in [15]. A surface level is defined, and the net buoyance force on a partly submerged element is computed from the geometrical considerations of a plane at a fixed height (z coordinate). Figure 2 illustrates the some of the fluid induced forces and internal forces in a three pipes domain.
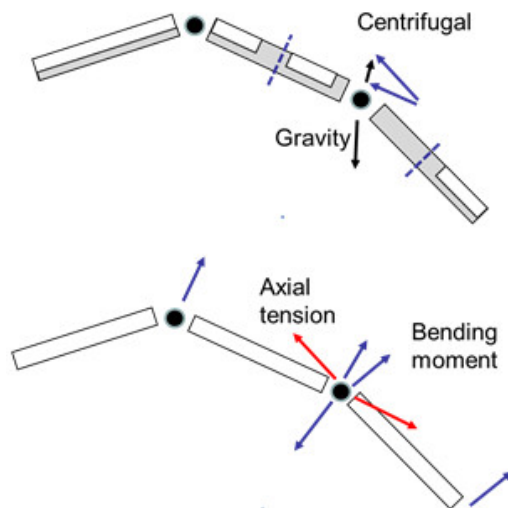

Figure 2. Data structure for the structural model. Forces from axial tension (red) and from bending moments (blue) gives the acceleration of the lumped mass elements. The main contributions from the internal flow are the gravity (average mass from each side) and change in momentum (centrifugal).

The implementation is vector based, using dot products and cross products on force and velocity vectors. This also made it quite straight forward to go to three dimensional pipe coordinates from a two dimensional scheme, by expanding the vectors and the operations.

The data structure has been designed such that the contributions of the forces from each side of a lumped mass are separate variables. This makes it easy to cut a pipeline, and continue the dynamic computations with two independent parts.

COUPLING

The time integration of the flow model and the structural model is managed in the same framework. The forces in the structural computation now gets contributions from the internal flow, mainly a change in

the gravitational force (mass of the gas-liquid mixture) and a centrifugal force (change in velocity directions).

After the structural displacement computations, the pipeline has a new shape. The simplest way is just to proceed as before, whereby the borders automatically get the updated pipe geometry through the links. A more complete coupling would be to also include the contributions of the axial component of the force from an accelerating pipe on the liquid flow inside.

The difference in time scales of the pipe and the flow dynamics, and also in the time integration methods, means that the time step is much lower for the structural computations, and a time step management is made accordingly. Several time steps are made with the structure solver for each time step in the flow solver.

EXPERIMENTAL SETUP

The experimental setup consisted mainly of an air tank of 0.04 m^3, valves, a flexible silicon hose, buoyancy modules and a 4x1.5x0.5 m water tank, assembled as in Figure 3. An air compressor is connected to the air tank through a needle valve (Valve A). A ball valve (Valve B) is fixed horizontally in the tank and connected to the air tank by rigid pipes. A pressure transducer is installed on the air tank. The water tank is filled until reaching Valve B.

Eight red marks are set along the hose at regular intervals of 300 mm starting at the same distance from the inlet. The hose can float on the surface when empty, but will sink when filled with water. A buoyancy module is set at the outlet of the hose, and a second buoyancy module is installed at 400 mm from the first one. Each buoyancy modules has a cylindrical shape with a hole in its axis for fitting the hose, external diameter of 52 mm and length of 50 mm.

A video camera was installed in front of the water tank and the pressure transducer was connected to a computer through a data acquisition board.

Valve B is closed and Valve A is open until the pressure in the air tank reaches a preset value. The hose is filled with water and the pig is inserted in the hose at 10 mm from the hose inlet, before connecting the hose to valve B. After the hose reached equilibrium and no waves may be observed on the free surface, the video camera and the logging software are activated. The experiment is started by rapidly opening valve B.

Table 1. Some properties of the pipe system

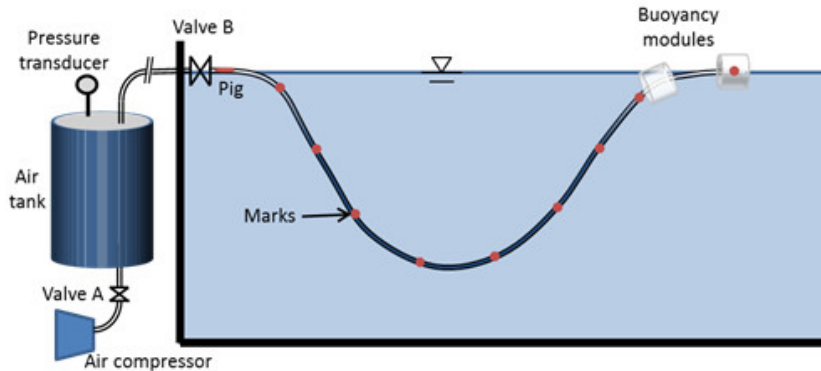|	
Length of rigid pipe (m)	5.45
Hose internal diameter (mm)	15.3
Hose wall thickness (mm)	3.25
Length of hose (m)	2.93
Linear mass density (kg/m)	0.23

Figure 3. Sketch showing the experimental setup

After the experiment is concluded, a text file containing values of air tank pressure (14 samples per second), and a video file (100 frames per second) of the test section are acquired. Three values of air pressure are tested: 25 kPa, 14 kPa and 10 kPa.

It involved some trial and error to arrive at a pig which would not stick to the wall (static friction) and also not give bypass flows of air or water. Pig of different materials, including expanded polystyrene, cork, rubber and Ethylene-vinyl acetate were tested. The final solution was a water filled small balloon. This balloon was seen to slide well along the pipe surface, and the balloon pressure would follow the upstream pressure and cause a good sealing with the wall. In the absence of a good pig launcher, a blow-out case was selected. This has well defined initial conditions, and can give a dramatic response of the pipe when the back pressure is increased.

NUMERICAL SETUP

The structural domain upstream Valve B is simplified as three horizontal pipes, the first of them being the air tank. The flexible hose is discretized in 117 elements of 25 mm each. An elastic modulus of 3.6 MPa is used, as the initial equilibrium shape is accurately reproduced. The external diameter of the hose is set to 21.8 mm. The length and internal diameter of all structural elements are presented in Table 2.

Table 2. Length and internal diameter of structural elements

Pipe number	Description	Internal Diameter (mm)	Length (mm)
1	Air tank	380.0	350
2	Pipe	16.0	3000
3	Valve B	15.3	50
4-100	Bare hose	15.3	25
101-102	Hose and buoy	15.3	25
103-118	Bare hose	15.3	25
119-120	Hose and buoy	15.3	25

All the degrees of freedom of pipes 1, 2 and 3 are fixed to ground. The rest of the nodes are constrained to move in the vertical plane.

In order to reproduce the experimental initial conditions, pipes 1, 2 and 3 are set as air filled at 25, 14 or 10 kPa, a pig section of 25 mm long is set in pipe 4 and a liquid slug is created from the pig front to the outlet.

The maximum fluid and structure solver time steps are set to 1e-3 and 1e-5 seconds respectively. The simulations are run for three seconds and the pig release time is set to 0.1 s.

RESULTS

The air tank pressure, pig position along the hose and hose displacement are extracted from experimental recordings and simulation result files for the three studied cases. Each case will be discussed separately in the following.

Case 1: Initial pressure of 25 kPa

Pig position along the hose and pressure at the air tank are plotted on Figure 4 and Figure 5 respectively. Both figures show good agreement between experiment and simulation results. The pig leaves the pipe after 1.12 s.
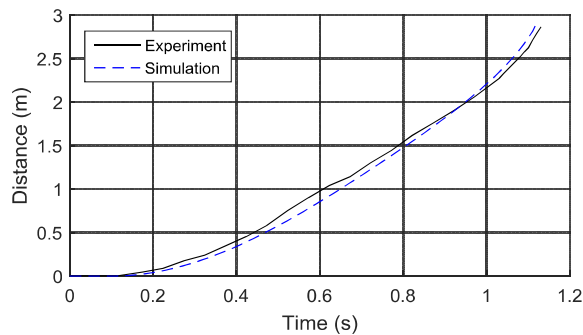
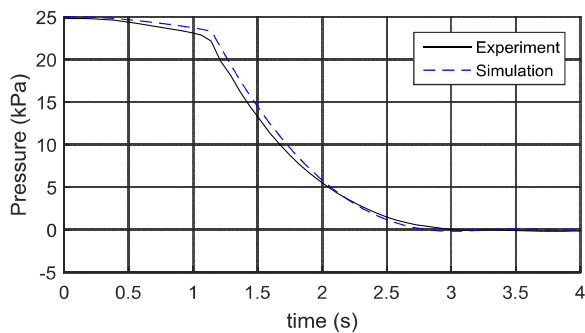**Figure 4. Pig location along the hose for case 1.**

Figure 5. Pressure at the air tank for Case 1.

Figure 6 shows the initial hose geometry as well as three other times instants before the pig is expelled. The pig location at the experiment is exposed by the arrow on each case in Figure 6.
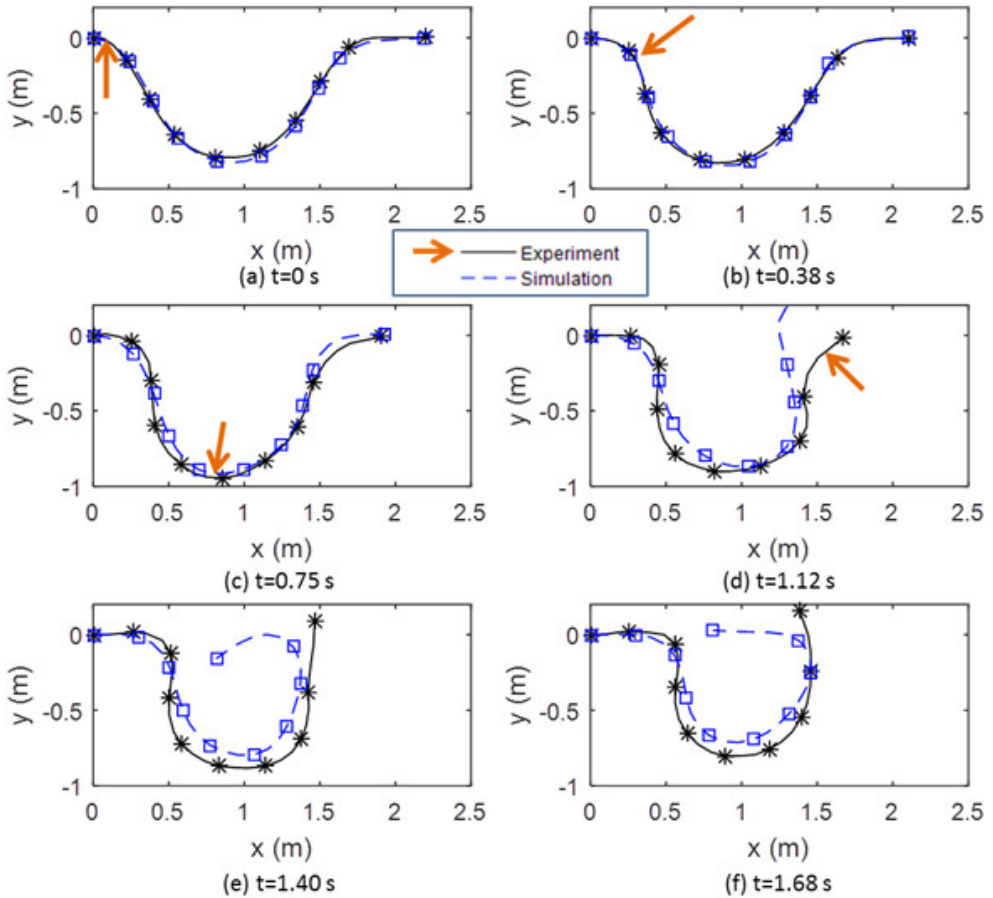
Figure 6. Hose shape and pig location at different time instants for case 1.
The arrows show the location of the pig on the experimental curve.

The behavior of the hose during the experiment is as follows: When the pig starts to move, the flow induced forces will tend to straighten out the first part of the U shaped pipe, lifting marks 1 and 2, and sinking marks 5, 6, 7 and 8 (Figure 6(b)). Marks 3, 4 and 9 present a mostly horizontal displacement. When the pig passes the bend just before mark 5 (Figure 6(c)), the vertical velocities of most of the marks has reduced almost to zero and soon turn into upward velocity. As the pipe pass thought mark 6, the effects of flow induced forces seem to have a limited impact, increasing the curvature of the bends between marks 7, 8 and 9. The pig is ejected and the pipe filled with only air rises. Mark 9 describes a curved trajectory as it moves over mark 8 (Figure 6(f)). At this moment, the hose is already in a 3D configuration, with the buoyancy elements touching the rear wall of the tank. The second buoyancy element keeps moving to the left and falls on the free surface next to mark 2.

Simulation results show that the initial condition is well reproduced (Figure 6(a)), as well as the first 0.7s. After that point, the predicted geometry of the hose between marks 8 and 9 deviates from the observed behavior. In Figure 6(d) the curvature of the U is over-predicted as one of the buoyancy units moves with almost no external resistance due to the negligible density above the water surface (Figure 6(e) and (f)).

Case 2: Initial pressure of 14 kPa

The predicted pig location along the hose and air tank pressure exhibit a delay of approximately 0.2 seconds compared with experimental measurements, as shown in Figure 7 and Figure 8. As the pressure behind the pig is reduced, its speed is also reduced, causing longer residence time.
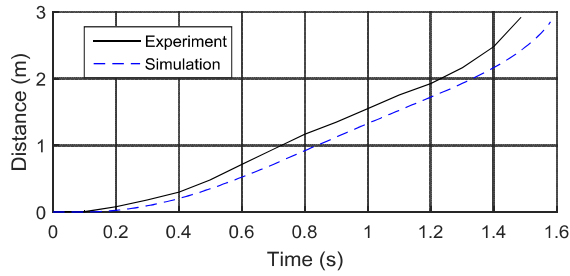

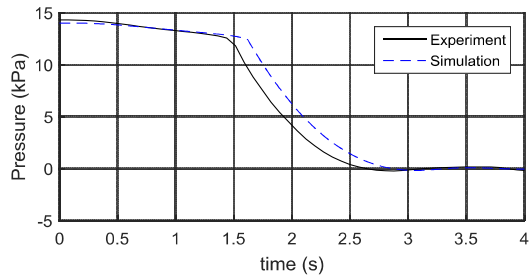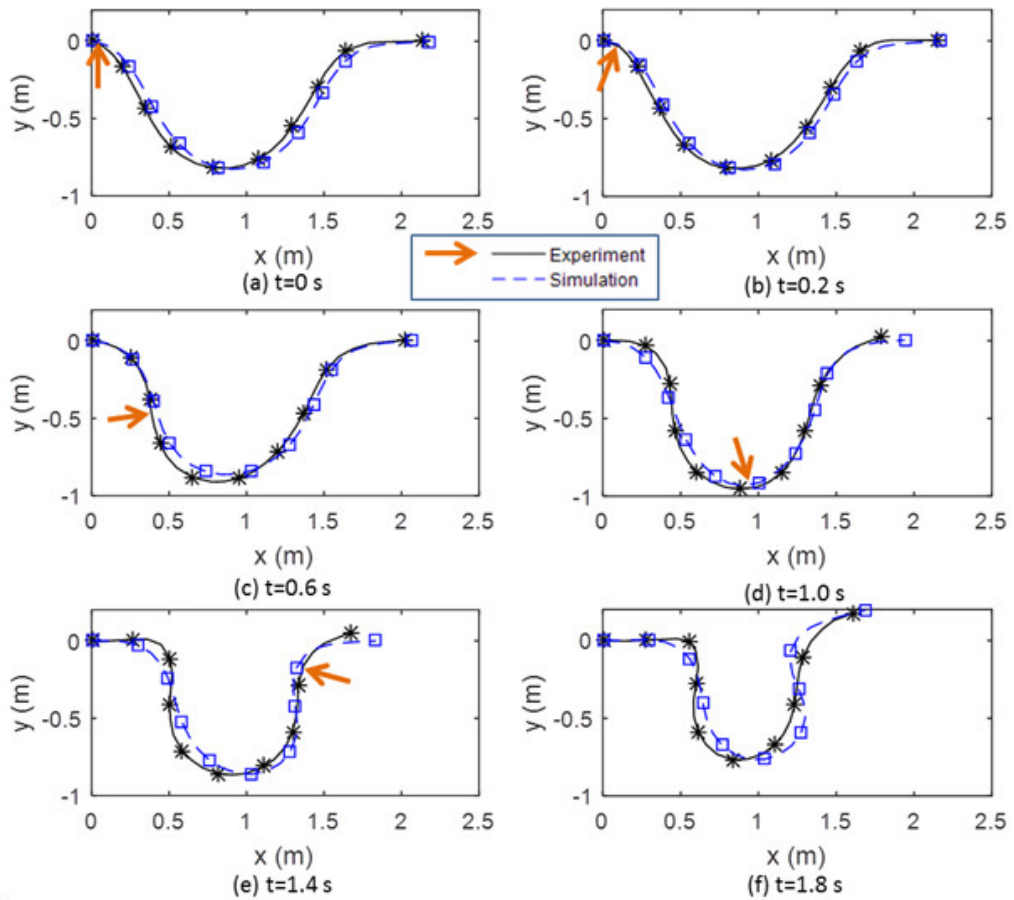**Figure 7. Pig location along the hose for case 2.**

Figure 8. Pressure at the air tank for Case 2.

The shapes of the hose for 6 different times are shown in Figure 9.

Figure 9. Hose shape and pig location at different time instants for case 2. The arrows show the location of the pig on the experimental curve.

Simulation results reproduce fairly well the behavior of the hose along the experiment. Figure 9(f) shows mark 9 over the water surface for both curves. Mark 9 falls back to the water surface at the right of mark 8 for experiment and simulation.

Case 3: Initial pressure of 10 kPa

The model predicts a 0.4 s shorter pig residence time compared with the experiment as presented in Figure 10.
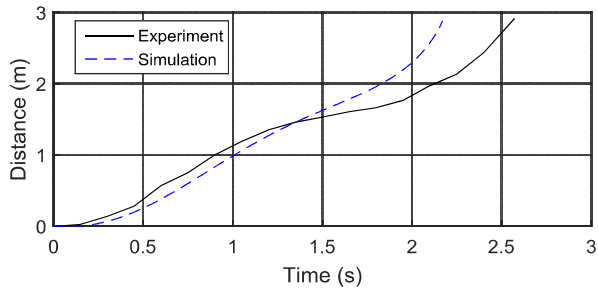
Figure 10. Pig location along the hose for case 3.

The speed of the pig reduces considerably before reaching the lowest point in the hose during the experiment. The speed reduction is less significant in the simulations as shown in Figure 11.
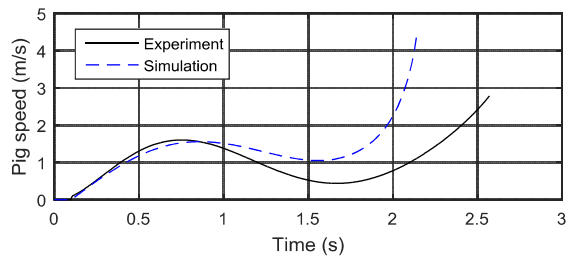

Figure 11. Pig speed for case 3.

As the pig advances through the hose, the internal density reduces, making the hose lift reducing the curvature of the U as depicted in the series of plots in Figure 12.
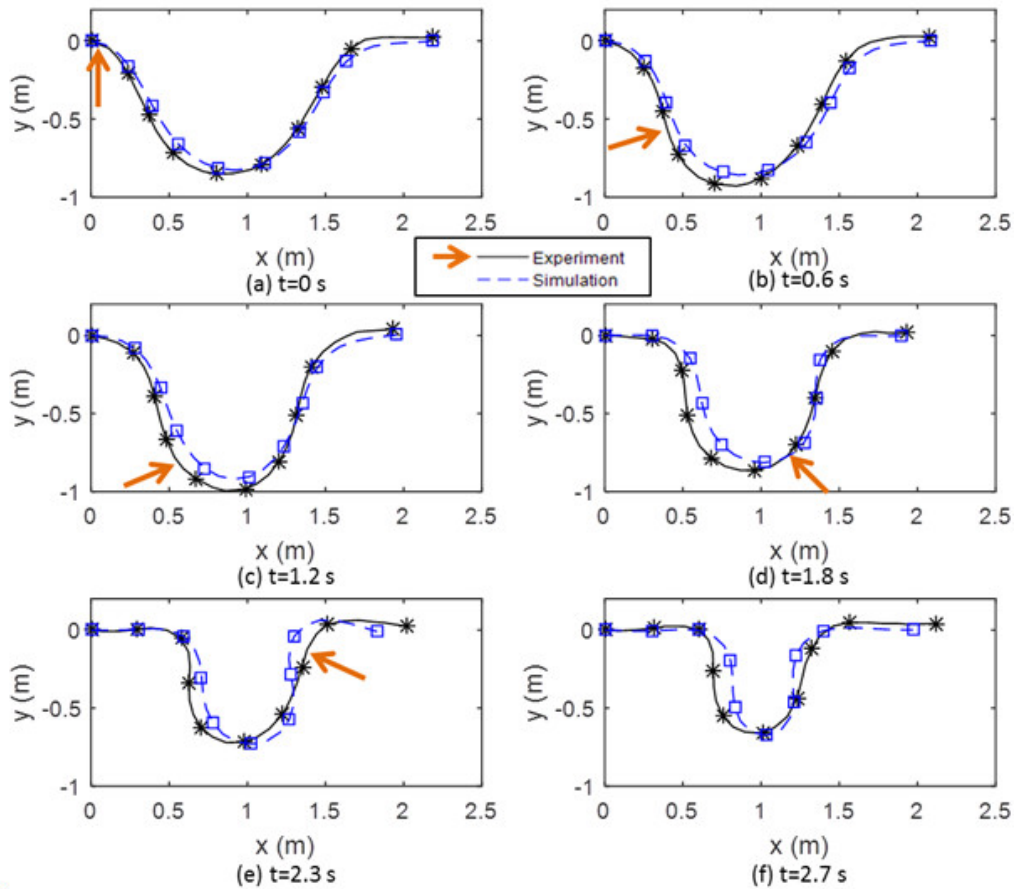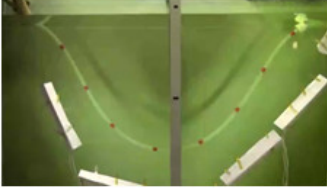
Figure 12. Hose shape and pig location at different time instants for case 3. The arrows show the location of the pig on the experimental curve.

Figure 13 shows some snap shots from the videos for case 1, where the pipe rises above the surface after the pig leaves, and for case 3, where the pipe stays submerged during the experiment.
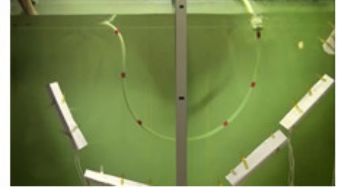
Case 1, 25 kPa pressure
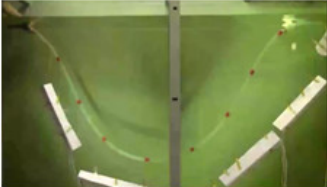
Initial water filled, pig at inlet　　　Pig is half way　　　Pig has left, pipe rising

Case 3, 10 kPa pressure

Initial water filled, pig at inlet　　　Pig is half way　　　Pig has left, pipe is straightening

Figure 13. Snapshots from video recordings of the experiments. Case 1 and case 3.

CONCLUSIONS

A two-way fluid structure interaction model is tested on a case with a pig driving out the liquid in a submerged, free hanging flexible pipe. The blow out is tested for three different back pressures of air. At the highest pressure, the pipe rises out of the surface, as a result of lift force on buoyancy elements, and falls back on the left side. At the intermediate pressure it falls on the right side and for the low pressure case, the pipe does not rise above the surface. The same behavior is seen in the coupled simulations. Fairly good agreement is obtained for the internal flow and the pig motion. The predicted structural dynamics of the hose shows larger deviations from the observed motion for larger initial pressures.

The discontinuity of the external density across the surface and the presence of the buoyancy modules increase the complexity of the problem, as drag and added mass forces may undergo large variations for small vertical displacements around the free surface. A more detailed analysis would then require a coupling to an external hydrodynamic flow model as well.

REFERENCES

[1]　C. M. Larsen, "Flexible riser analysis — comparison of results from computer programs," *Marine Structures,* vol. 5, pp. 103-119, 1992.
[2]　V. Tin, "Severe Slugging in Flexible Risers," presented at the 5th International Conference on Multiphase Production, Cannes, France, 1991.
[3]　O. J. Nydal, M. Audibert, and M. Johansen, "Experiments and modelling of gas-liquid flow in S-shaped riser," presented at the 10th International conference on multiphase production, Cannes, 2001.
[4]　J. A. Montgomery and H. C. Yeung, "The Stability of Fluid Production From a Flexible Riser," *Journal of Energy Resources Technology,* vol. 124, pp. 83-89, 2002.

[5]   M. J. C. Diaz, M. Khatibi, and O. J. Nydal, "Severe Slugging With Viscous Liquids: Experiments and Simulations," presented at the 9th North American Conference on Multiphase Technology, Banff, Canada, 2014.

[6]   W. Li, L. Guo, and X. Xie, "Effects of a long pipeline on severe slugging in an S-shaped riser," *Chemical Engineering Science,* vol. 171, pp. 379-390, 2017.

[7]   A. Ortega, A. Rivera, O. J. Nydal, and C. M. Larsen, "On the Dynamic Response of Flexible Risers Caused by Internal Slug Flow," presented at the 31st International Conference on Ocean, Offshore and Arctic Engineering, Rio de Janeiro, Brazil, 2012.

[8]   A. Ortega, A. Rivera, and C. M. Larsen, "Slug Flow and Waves Induced Motions in Flexible Riser," *Journal of Offshore Mechanics and Arctic Engineering,* vol. 140, 2017.

[9]   J. J. Vieiro, A. Hemeda, and O. J. Nydal, "Experimental and Numerical Simulation of two-phase flow and structural dynamic of a collapsed flexible pipe on the seabed," presented at the International conference on the Advances in Subsea Engineering, Structures and Systems, Glasgow, United Kingdom, 2016.

[10]   J. J. Vieiro, E. Ita, and O. J. Nydal, "Two-Way Fluid-Structure Interaction in a Flexible Pipe Conveying Gas-Liquid Slug Flow," presented at the OTC Brasil 2015, Rio de Janeiro, Brazil, 2015.

[11]   J. J. Vieiro, A. Hemeda, and O. J. Nydal, "Multiphase Flow in Flexible Pipes: Coupled Dynamic Simulations and Small Scale Experiments on Garden Hose Instability," presented at the Eighth National Conference on Computational Mechanics, MekIT'15, Trondheim, Norway, 2014.

[12]   I. E. Smith and O. J. Nydal, "The effect of boundary conditions and droplet entrainment on severe slugging using a Lagrangian slug tracking model," *International Journal of Multiphase Flow,* vol. 85, pp. 245-257, 2016.

[13]   T. K. Kjeldby, R. A. W. M. Henkes, and O. J. Nydal, "Lagrangian slug flow modeling and sensitivity on hydrodynamic slug initiation methods in a severe slugging case," *International Journal of Multiphase Flow,* vol. 53, pp. 29-39, 2013.

[14]   O. J. Nydal, "Dynamic Models in Multiphase Flow," *Energy & Fuels,* vol. 26, pp. 4117-4123, 2012.

[15]   R. Ghadimi, "A simple and efficient algorithm for the static and dynamic analysis of flexible marine risers," *Computers & Structures,* vol. 29, pp. 541-555, 1988.